# SYNTHESIS, CHARACTERIZATION AND APPLICATION OF BIMETALLIC-BASED NANOCOMPOSITES FOR HYDROCRACKING OF NAPHTHALENE

BY

**TAYE DAMOLA SHUAIB**

A Thesis Presented to the
DEANSHIP OF GRADUATE STUDIES

**KING FAHD UNIVERSITY OF PETROLEUM & MINERALS**

DHAHRAN, SAUDI ARABIA

In Partial Fulfillment of the
Requirements for the Degree of

## MASTER OF SCIENCE

In

CHEMISTRY

MAY, 2015

KING FAHD UNIVERSITY OF PETROLEUM & MINERALS

DHAHRAN- 31261, SAUDI ARABIA

**DEANSHIP OF GRADUATE STUDIES**

This thesis, written by **DAMOLA TAYE SHUAIB** under the direction of his thesis advisor and approved by his thesis committee, has been presented and accepted by the Dean of Graduate Studies, in partial fulfillment of the requirements for the degree of **MASTER OF SCIENCE IN CHEMISTRY.**

Dr. Tawfik A. Saleh
(Advisor)

Dr. Abdul-Aziz A. Al-Saadi
Department Chairman

Dr. Mohammed A. Al-Daous
(Member)

Dr. Salam A. Zummo
Dean of Graduate Studies

Dr. Oweimreen Ghassan
(Member)

3/6/15
Date

*Dedication*

This work is dedicated to my family

# ACKNOWLEDGMENTS

My sincere appreciation goes to the good people of Chemistry Department, King Fahd University of Petroleum & Minerals (KFUPM). My deep gratitude is extended to the Center of Excellence in Nanotechnology (CENT), Center for Environment and Water (CEW), Department of Physics for their support for different analyses towards making this research a success.

With deep sense of gratitude, I would like to thank my advisor in person of Dr. Tawfik Abdo Saleh for his inspiring guidance and excellent cooperation in supervising this research work. I am also very grateful to Dr Mohammed A. Al-Daous of Saudi Aramco Oil Company and Professor Ghassan Oweimreen, who are members of my research committee, for facilitating this research, constant encouragement and several discussions.

My profound gratitude also goes to Mr Darwin (Chemistry Department), Mr Hatim, Mr Ricardo (CEW-RI), Mr Abdulkeem Akinpelu and Mr Lui Litorja (CEW-RI) for their favors in one way or the other. My Special thanks to my research group's members Gaddafi and Muatesem. Friends like Abdulazeez, Kazeem, Aliyu, Babatunde, Olakunle and others too numerous to mention.

Finally and humbly, I offer my sincere thanks to my parent, wife and other family members especially my twin brother for their encouragement and prayers

# TABLE OF CONTENTS

# LIST OF TABLES

# LIST OF FIGURES

# LIST OF ABBREVIATIONS

HYD : Hydrogenation

HYC : Hydrocracking

HDS : Hydrodesulfurization

HDN : Hydrodenitrogenation

CN : Cetane number

RuECY-B : Ruthenium exchanged calcined Y-zeolite B-series catalyst

Ru-$Al_2O_3$_YD : Ruthenium supported on alumina-coated Y-zeolite D-series catalyst

PdECY-B : Palladium exchanged calcined Y-zeolite B-series catalyst

Pd-$Al_2O_3$_YD : Palladium supported on alumina-coated Y-zeolite D- Series catalyst

RuPdECY-B : Ruthenium-Palladium exchanged calcined Y-zeolite B-series catalyst

RuPd- $Al_2O_3$_YD: Ruthenium-Palladium exchanged calcined Y-zeolite D-series catalyst

DBT : Dibenzothiophene

SEM : Scanning Electron Microscopy

TEM : Transmission Electron Microscopy

STEM : Scanning Transmission Electron Microscopy

TPR : Temperature-Programmed Reduction

PXRD : Powder X-Ray Diffraction

# ABSTRACT (ENGLISH)

Full Name : [TAYE DAMOLA SHUAIB]

Thesis Title : [SYNTHESIS, CHARACTERIZATION AND APPLICATION OF BIMETALLIC-BASED NANOCOMPOSITES FOR HYDROCRACKING OF NAPHTHALENE]

Major Field : [CHEMISTRY]

Date of Degree: [MAY, 2015]

Different series of bimetallic-based catalysts (RuPdECYB and RuPd-$Al_2O_3$_YD) composed of varying amounts of Ru-Pd nanoparticles supported on naked and alumina-coated Y-zeolite were developed and characterized by PXRD, SEM, TEM, EDX, ICP-OES, $H_2$ chemisorptions and TPR experiments. The crystalline metal particles are well dispersed and stabilized on the supports. These materials proved to be versatile for the liquid-phase hydrocracking of poly-cyclic aromatic hydrocarbons (naphthalene) and S-heteroaromatics (dibenzothiophene) which are representative components of petroleum-derived fuels, under moderate reaction conditions. The effect of metal loading on conversion of naphthalene was observed to be linear and the nature of supports affects product distribution and yield. The catalysts with naked Y-Zeolite support yielded more cracking products (Monoaromatics and Cyclohexanes) than alumina-coated Y-Zeolite supported catalysts due to the more acidic nature

On the contrary, the coated series of catalysts were more selective towards hydrogenation products (Tetralin and Decalins). The faster rate of hydrogenation

process than cracking further confirmed the higher yield and selectivity of all the tested catalysts to Tetralin and Decalins. All the prepared catalysts were very stable and regenerable which indicate their re-usability without any appreciable loss of catalytic activity, even in the presence of catalyst's poison-containing dibenzothiophene (DBT). A maximum conversion of 88.3 % of naphthalene was achieved on ruthenium single metal-based catalyst and 86.4 % for Ru-Pd bimetallic-based catalyst. With Pd single metal catalyst, the conversion achieved was less than 20 % which is slightly higher than what is observed for bare supports employed in this study. Nonetheless, the thio-tolerant activity was better with bimetallic catalyst than single metal Ru catalyst. This could be confirming the promotional effect of metals in a bimetallic system. The pore-size of the catalyst's support, optimum metal loading and acidity are key factors to be considered for future designs of new, efficient and poison-resistant metal catalyst system for hydrocracking process.

# ABSTRACT (ARABIC)


**ملخص الرسالة**

**الاسم الكامل: دامولا تاي شعيب**

**عنوان الرسالة: تحضير وتوصيف مخاليط نانوية ثنائية المعادن وتطبيقاتها في التفكيك الهيدروجيني للنفثالين**

**التخصص: كيمياء**

**تاريخ الدرجة العلمية: مايو 2015**

**لقد تم تحضير مجموعتين من المواد الحافزة مكونة من معدني الروثينيوم والبلاديوم مدعمة على سطح الزيوليت. تم استخدام كميات مختلفة من جسيمات الروثينيوم والبلاديوم النانومترية. كما تم استخدام نوعين من أسطح الزيوليت وهما زيوليت واي والزيوليت المعامل بأكسيد الألمنيوم. تم توصيف المواد المحضرة عن طريق مطيافية المسح الالكتروني ومطيافية الانتقالات الالكترونية ومطيافية الذرة وتشتت اشعة اكس والاختزال الحراري المبرمج وجهاز مطياف القياس بالبلازما وغيرها. أثبتت نتائج التوصيف أن جسيمات المعادن البلورية توزعت بشكل شبه متجانس وثابت على سطح الزيوليت. هذا وقد أثبتت التجارب فاعلية هذه المواد فى التكسير الهيدروجينى فى الحالة السائلة تحت ظروف التفاعل العادية لمركبات الوقود المشتقة من البترول سواء الهيدروكربونات الأروماتية عديدة الحلقات مثل النفثالين، أو المركبات الأروماتية الغير متجانسة مثل داي بنزو ثيوفين. كما ثبت أن تكسير النفثالين يعتمد على كمية المعدن المستخدم بعلاقة خطية؛ بالإضافة إلى أن كمية ونوعية الناتج النهائي تعتمد على طبيعة سطح الزيوليت المستخدم، حيث أثبتت التجارب أن العامل الحفاز المحّمل على الزيوليت الغير مطلي بالألومينا قد قام بتكسير النفثالين إلى عدد من المركبات (مركبات أروماتية وحيدة الحلقة وهكسان حلقي) أكبر من تلك التى تكونت فى حالة استخدام زيوليت مطلي بالألومينا بسبب زيادة الحامضية فى حالة عدم طلاء الزيوليت. إلا أنه قد أثبتت التجارب أن العوامل الحفازة المحّملة على الزيوليت المطلى بالألومينا أكثر**

**إنتاجاً للمركبات المشبعة بالهيدروجين (تيترالين وديكالين)، حيث أن معدل عملية الهدرجة كان أعلى بكثير من معدل التكسير أو التفكيك.**

**جدير بالذكر أن كل العوامل الحفازة التى تم تحضيرها أظهرت ثباتاً وقابلية للاستخدام أكثر من مرة دون تأثر فاعلية الحفز، حتى فى وجود المركبات التى قد تقلل من كفاءة العامل الحفاز مثل داى بنزو ثيوفين. هذا وقد تم تحويل حوالي 88.3% من النفثالين باستخدام الروثينيوم فقط، مقارنة ب 86.4% في حالة الروثينيوم والبالاديوم؛ إلا أنه عند استخدام البالاديوم فقط، تم تحويل أقل من 20% من النفثالين وهي نسبة أعلى بقليل من تلك التى تم تحويلها فى حالة عدم طلاء الزيوليت. هذا وقد أثبتت التجارب أن فاعلية العوامل الحفازة التي تعتمد على معدنين تجاه المركبات التي تحتوي على عنصر الكبريت أفضل من تلك التي تعتمد على الروثينيوم فقط، مما يؤكد التأثير الفعال الناجم عن استخدام معدنين. وأخيراً عند تصميم عامل حافز معدني، فعال، مقاوم للمركبات التى تقلل من معدل الحفز لاستخدامه فى عمليات التكسير الهيدروجينى؛ فإنه يجب مراعاة أكثر من متغير مثل حجم مسام السطح الذي يتم تحميل العامل الحفاز عليه، كمية العامل الحفاز المستخدمة، ودرجة الحامضية.**

# CHAPTER 1

# INTRODUCTION

## 1.1 Background Information

The roles of catalysis are fundamental in industrial technological development. These roles are scientifically, technically and practically vital to refiners and chemical industries. The increasingly stringent environmental policies on the use of transportation fuels with ultra low aromatics and sulfur contents in order to improve air quality has contributed to the high global research focus on catalysts for hydrotreating of polyaromatic hydrocarbons (PAHs) which are found mostly in heavy oils [1,2]. In order to enhance the performance of combustion engine and achieve increased cetane number (CN) which is a reference index for measuring ease of ignition of hydrocarbons when compressed and cetane (hexadecane) is assigned CN of 100 [1-3]. Hydrogenation of PAHs is an effective way of producing cycloalkanes (stable jet fuel) thus decreasing aromatic contents and consequently enhanced CN. Hydrogenation, to a very high degree, is a very vital unit operation in petroleum refining [3].

On the other hand, the need to produce more volume of hydrocarbons to meet up with global market demands has necessitated the conversion of low grade feed-stocks like heavy oil and light cycle oils (LCO; naphthalene) through catalytic cracking to transportation fuels and other feed-stocks used in chemical industry. This, however, is

challenging but with enormous economic gain. The tremendous growth and development in the area of material science in the last two decades have brought into limelight great innovations in the area of catalytic processes. Quite a large number of porous solid materials have been developed that are of high industrial benefits.

In any catalyzed reaction, the reactant(s) get in contact with the surface of the catalyst by diffusing through its pores for reaction to take place. This diffusion governs the overall rate of chemical reactions. The nature of the molecules and their interaction with their surroundings depicts the mechanisms through which diffusion may proceed [4]. In a heterogeneous reaction, the following order is expected:

(a) External surface diffusion of reactants from the flowing stream to the crystal surface (of the catalyst).

(b) Internal diffusion of the reactants through the pores of the catalyst.

(c) Adsorption via collision of the reactants on the l active sites crystal,

(d) Interaction (physical and chemical) between the reactant molecules and active sites of the catalyst.

(e) Desorption of the resultant products from the active sites.

(f) Diffusion of resulting products via the pores of the crystal to its external surface.

(g) Movement of the final products from the external surface of the crystal into the reaction stream.

## 1.2 Desire for Hydrocracking Catalysts

The tremendous growth of hydrocracking process over the past years can be traced to its flexibility employs in refining petroleum. This process has been used extensively in converting feedstocks (e.g petroleum residue and Naphtha) to desirable products of better values such as lubricating oils, kerosene, jet fuels, middle distillates, gasoline, industrial chemicals e.t.c These products are, in addition, of lower boiling points than the feed.

Several low-cost and versatile hydrocracking catalyst systems that can withstand harsh operating conditions have been established. Factors such as feed and product properties, hydrocracking unit capacity, economic considerations among others determine the choice of catalyst for the desired process. Hydrocracking process can be carried out commercially in a single stage or two stages. Figure 1 below shows a simple schematic representation of hydrocracking process [5].

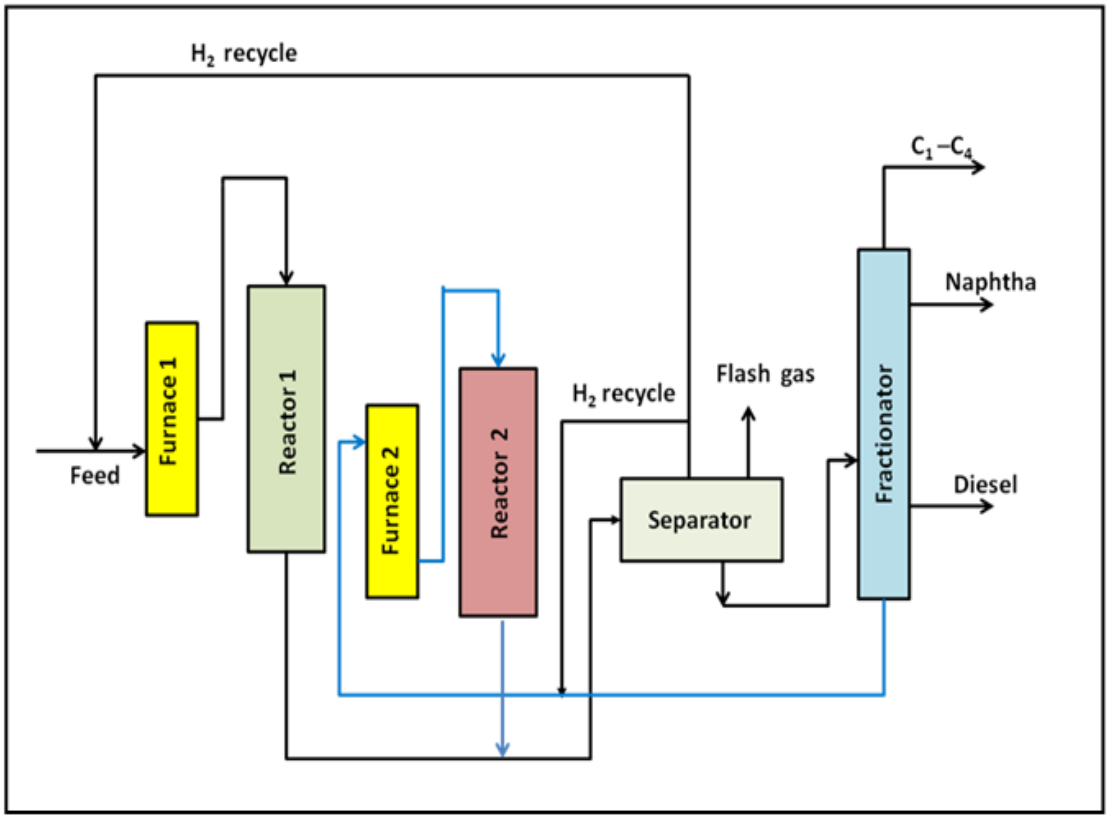


**Figure 1.1 A schematic representation of two-stage hydrocracking process**

## 1.3 Hydrocracking Chemistry

Catalytic processes via heterogeneous solid are very vital to petroleum refining industry. The major processes are depicted in figure 1.2 [6].

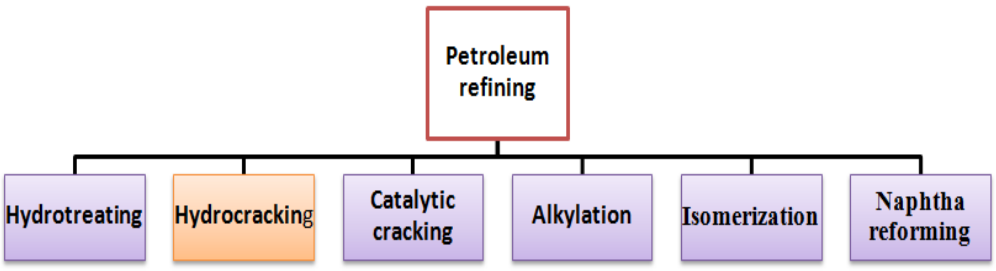


**Figure 1.2** Petroleum refining catalytic processes via solid catalyst

The following are three major routes followed during hydrocracking reactions:

1. Hydropyrolysis i.e. a non-catalytic thermal cleavage of carbon-to-carbon bond via hydrocarbon radicals and addition of hydrogen.
2. Hydrogenolysis i.e. a carbon-to-carbon bond cleavage over hydrogenation composites (Ru, Pt, Ir, Pd, Ni, Mo, Co, oxides, or sulfides) alongside hydrogen addition.
3. Carbon-to-carbon bond cleavage with addition of hydrogen via bifunctional catalyst consisting of hydrogenation material on porous acidic support [4, 5]. This last route is the most common for hydrocracking processes in petroleum refining and also the focus of this research.

Hydrotreating processes are other reactions occurring during hydrocracking processes. These include; hydrodenitrogenation (HDN) for nitrogen removal, hydrodesulfurization (HDS) for sulfur removal, partial aromatics saturation, olefin hydrogenation, hydro-deoxygenation (HDO) for oxygen removal etc.

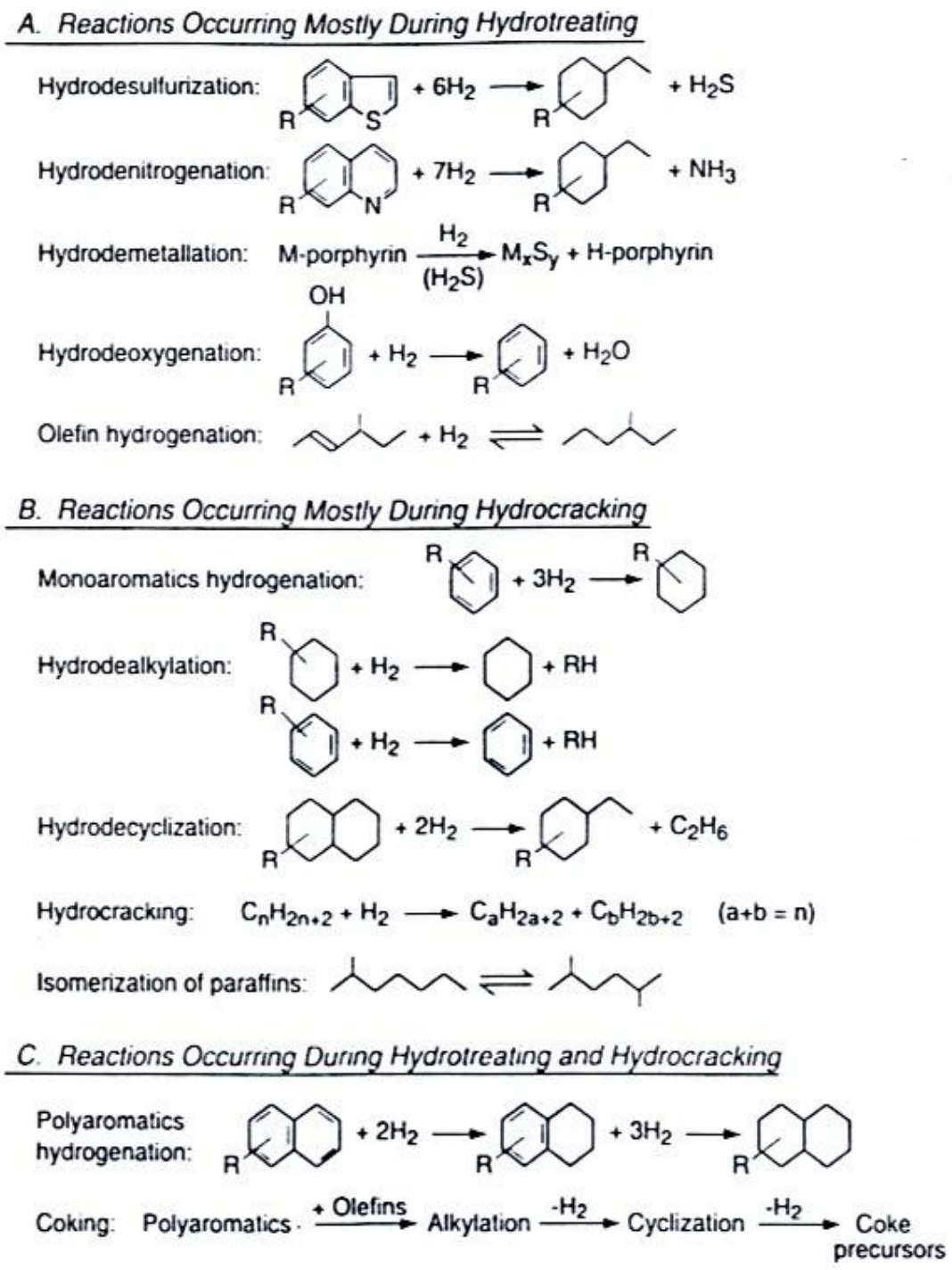


**Figure 1.3** Typical hydrocracking reactions [8]

A better understanding of hydrocracking chemistry can be achieved by studying its kinetics for various feedstocks used industrially [5, 6, 7, 9]. For a well detailed kinetic

model for gas oil cracking, several reaction steps that are elementary in nature are involved; this gives rise to a very complex kinetics which is extremely difficult to follow. In order to simplify this, the reaction steps and products are assigned into groups which are referred to as lumps and are independent entity. This is referred to as lumped kinetics approach.

For gas oil cracking, three lumped model was proposed with one path producing gasoline /diesel and the second path yielding gases/coke both occurring in first order with respect to each hydrocarbon feed. Gas and coke can further be formed from gasoline/diesel as depicted in figure 1-3.

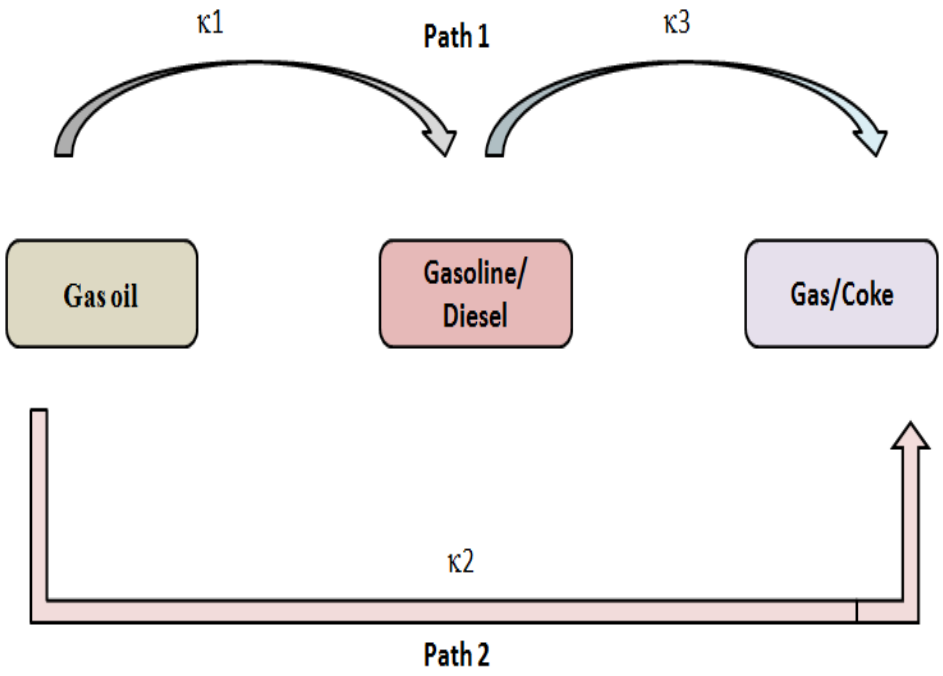


**Figure 1.4** Three Lumped kinetic model for catalytic cracking of gas oil [10].

## 1.4 Role of Hydrotreating Catalysts

Hydrotreating provides means of getting rid of hetero atoms present in crude oil. It is catalytic process that removes hydrogen, cleaves carbon-to-carbon bonds and the same time adds hydrogen to feedstocks. This processes removes sulfur (the most abundant hetero-atom in fuel oil), nitrogen, oxygen, metal and other constituents. In the presence of appropriate catalyst and hydrogen, hydrotreating is an integral part of a complex operation for removing undesired species and lower the molecular weight of heavy of petroleum feedstocks.

### 1.4.1 Hydrodesulfurization (HDS)

Compounds of sulfur in crude oil are the most abundant heteroatomic organo-compounds which their removal is very challenging and pose a great danger to the environment. Sulfur compounds are known to poison catalysts employ in petroleum refining process. These organosulfur compounds are present as thiols, thiophene and its derivatives, sulfides e.t.c.

During the process of desulfurization, sulfur compounds, for instance, benzothiophene or dibenzothiophene are removed from the stream and then decomposed separately in a vessel. A very low level of sulfur in transportation fuels can be achieved through this process [11]. This process provides an insight for removing sulfur compounds in fuels through distillation with the help of catalysts. It's also possible that some sulfur products (solid or gas) are generated with just decomposition of of organosulfur compounds with only the hydrocarbons (without sulfur) remaining in the process stream (example is hydro

desulfurization). The last class is just a simple removal of organosulfur compounds from process stream. This can be done by conversion of the organosulfur compounds to different compounds that can be removed easily if direct removal is difficult or impossible; however, disposal of the removed sulfur compounds becomes a great challenge for this type of class [11].

In HDS reactions, hydrogenation of thiols (mercaptans) and sulfides lead to the formation of hydrocarbons and hydrogen sulfides [12]. Some of these reactions are shown below:

| Sulfur Class | Reaction |
|---|---|
| Mercaptans | $R\text{-}SH + H_2 \longrightarrow RH + H_2S$ |
| Sulfides | $R\text{-}S\text{-}R + 2\ H_2 \longrightarrow 2\ RH + H_2S$ |
| Disulfides | $R\text{-}S\text{-}S\text{-}R + 3H_2 \longrightarrow 2\ RH + 2H_2S$ |
| Thiophene | 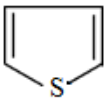 $+\ 4\ H_2 \longrightarrow CH_3(CH_2)_2CH_3 + H_2S$ |

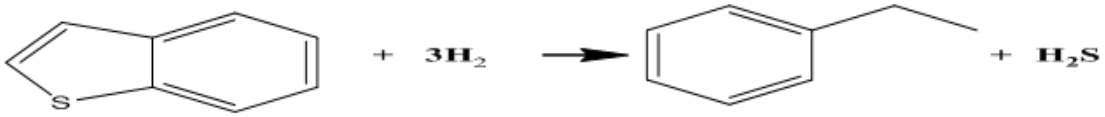

Benzothiophene

In the case of highly substitute dibenzothiophene, hydrocarbon is produced mainly via ring opening then sulfur extrudes out of the parent. The alkyl-substituents on the aromatic

ring of dibenzothiophene, especially the ones adjacent to sulfur atom, create steric hindrance which prevent adequate bond interaction with surface of the catalyst. This greatly affects Hydrodesulfurization process as necessary intermediates are not formed [13]. The details of HDS mechanism will be discussed in the next chapter.

## 1.5 Catalyst deactivation

Catalyst deactivation is a major problem in hydrocracking process. Some catalysts get poisoned easily and this drastically reduces their potency. A typical example is sulfur poisoning of hydrocracking catalysts. The following are the common sources of catalyst deactivation:

a. Coke formation
b. Sintering
c. Deactivation by metals such as Pt, Ni, V e.t.c

A major deactivation source of catalytic cracking is coke formation on its surface [4]. A low residence time in the reactor will be experienced if the amount of coke formed is high and this occurrence translates to a very high frequency for regeneration. The residual metals present in the feed also contribute to catalytic potency. As vanadium destroys zeolitic frame work which has negative effect on activity of the catalyst; nickel is known to elevate selectivity to coke and gas formation. The negative effects can be minimized or prevented by alloying nickel with bismuth or antimony (Ni-Bi or Ni-Sb). Either Antimony or bismuth compound can play a role of a passivator when added to forms Ni-

Sb or Ni- Bi alloy. Magnesium orthosilicate can also be added to trap vanadium as vanadium oxide in the form $MgO\text{-}V_2O_5\text{-}SiO_2$ [4, 7].

## 1.6 Research Objectives

The intent of this research work is summarized as follows:

1. Prepare hydrotreating catalysts with different supports in terms of porosity and acidity. These supports are:
    - Ultra Stable Y (USY) zeolite.
    - γ-alumina.
2. Introduce Ruthenium and Palladium by ion-exchange mechanism to the supports.
3. Test the hydrocracking efficacy of prepared catalysts with a model oil feed of Naphthalene dissolved in dodecane.
4. Compare the prepared catalysts activities with previously reported ones under similar conditions.
5. Evaluate the sulfur-tolerant ability of the developed catalysts.
6. Design simple kinetic model for the reactions.

# CHAPTER 2

# LITERATURE REVIEW

In designing hydrocracking catalysts, and especially for commercial application,

Bi-functional materials are most appropriate because of the dual sites of activity. The incorporation of hydrogenation/dehydrogenation (active metal sites) and cracking (acidic support) functionalities gives the desired dual nature. These bifunctional catalysts are very versatile and flexible in such a way that the two sites of activities can be maneuvered to achieve the desired product. The balance between the hydrogenation/dehydrogenation and acidic support components governs, to a large extent, the type of reactions happening and the products formed [8]. Table 2.1 summaries some previously reported hydrogenation and hydrocracking processes, reaction conditions and results achieved.

**Table 2.1 Some reported hydrogenation and hydrocracking processes and their parameters.**

| Type of support | Metal loaded/Weight (wt %) | Function | Feed (wt %) | Reaction conditions | Performance (%conversion) | Reference |
|---|---|---|---|---|---|---|
| H-Y zeolite | Ir(3.1)-Pt(4.0) | HYD/ HYC | Cis-decalin | 290-350 $^0$C 7.0 MPa | 98-99 | [14] |
| H-Y zeolite | $Mo_2C$(13) $Mo_2C$(27) | HYD/ HYC | Naphthalene | 300 $^0$C 3 MPa | 91 84 | [15] |
| Magnesia (MgO) | Ru(10) Ru(10) | HYD | Naphthalene (5mmol) & Anthracene (5mmol) Benzothiophene (5mmol) | 150 $^0$C 50 atm | 61(BT) | [16] |
| γ-alumina | F-Pt(0.4)- | HYD | Phenantren | 300 $^0$C | 81.5 | [17] |

| | | | | | | |
|---|---|---|---|---|---|---|
| | Pd(0.6) | | e(5)<br>Naphthalene(5)<br>Tetralin(5) | 500 psig | 85.1<br>50.9 | |
| γ-alumina | Ni(5)<br>NiW | HYD | Naphthalene | 350 $^0$C<br>3 MPa | 74.3<br>97.8 | [18] |
| Alumina-USY | NiMoS | HYD/<br>HYC | 1-methyl Naphthalene(10) | 360 $^0$C<br>5 MPa | 88.7 | [19] |
| Zirconium-doped Silica | Ru-Pd(5) | HYD/<br>HYC | Tetralin | 350 $^0$C<br>6 MPa | 98.5 | [20] |

HYD=hydrogenation; HYC= hydrocracking

Annotation is the same as in table 2.1

## 2.1 Composition and functionalities of hydrocracking catalysts

There are many acidic supports with good track records of activities in catalytic hydrocracking today. Among these acidic supports are; (i) silica-alumina (amorphous oxides) (ii) Y-zeolites (crystalline with alumina as binder), (iii) a mixture of both amorphous oxides and crystalline zeolites. Other supports are; different combinations of silica, alumina boria, titania, magnesia and other solid acids. Noble metals (ruthenium, palladium, platinum e.t.c) provide hydrogenation/dehydrogenation. Sulfides of group VIA (molybdenum ($MoS_2$), tungsten) and group VIIA (nickel, cobalt) .These metals enable the hydrogenation of the hydrocarbon feed, providing it for cracking, removal of heteroatom, formation of olefin intermediates through dehyhydrogenation and reduction of coke formation [21]. Some compositions and strength of acidity of bifunctional catalysts are as depicted in figure 2.1 and 2.2.

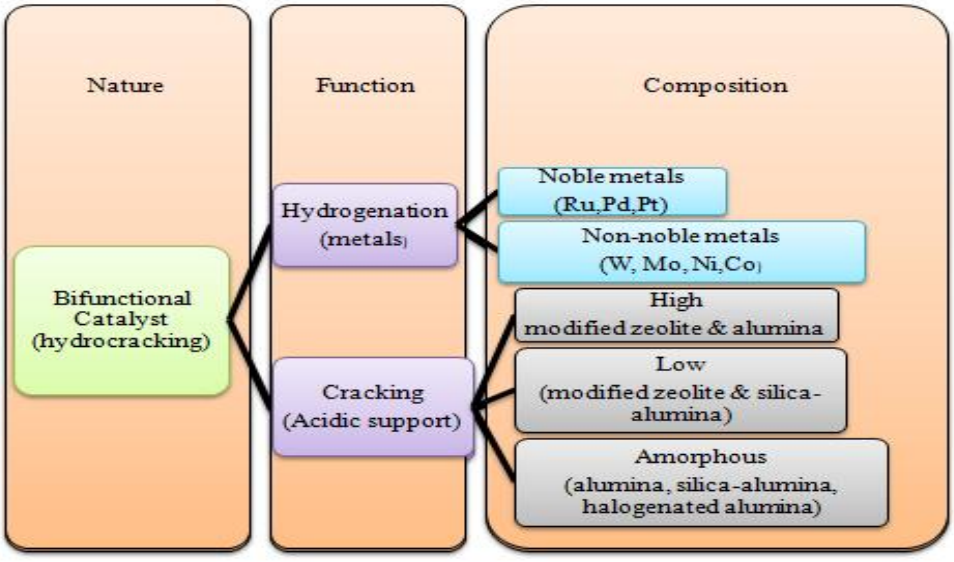


**Figure 2.1 Bifunctional catalysts compositions for hydrocracking process [8].**

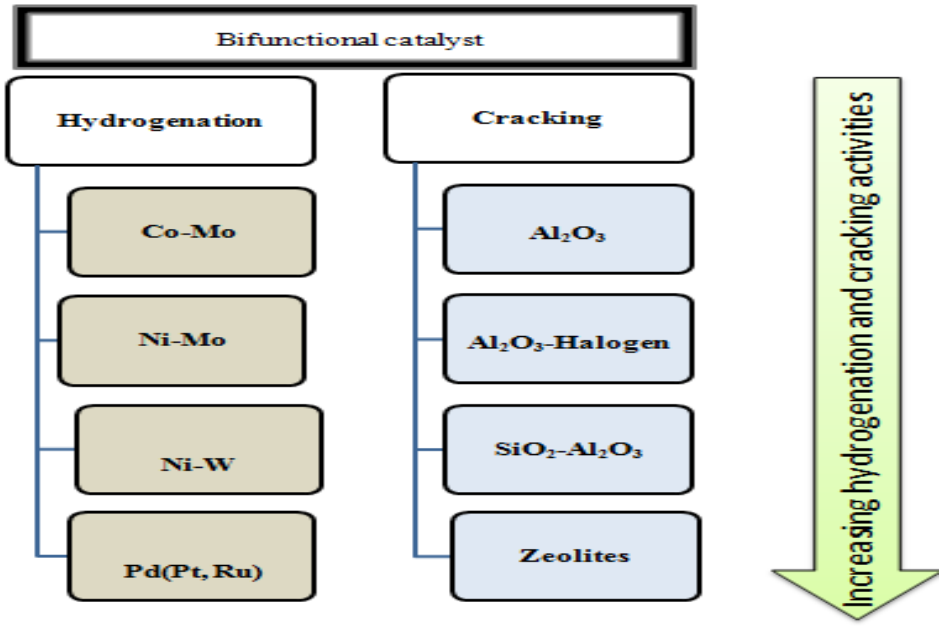


**Figure 2.1** Strength of Hydrogenation and Cracking Functions in Bi-functional Catalysts [8].

Due to the fact that feedstock in refinery stream contains sulfur compounds (hydrogen sulfide, thiophene, benzothiophene, dibenzothiophene), the metal sites are sulfided (e.g. nickel sulfide, cobalt sulfide) to enhance hydrotreating processes. The figure 2.3 below was obtained from toluene conversion in the presence of hydrogen sulfide presents the results obtained when toluene is used as a model molecule in the presence of hydrogen sulfide. It is obvious from the plot that a maximum conversion is reached for all the different combinations of metals when the atomic ratio is 0.25 [22]. However, adding more loads of these metals to the support does not translate to a significant increase in the catalytic activity [23].

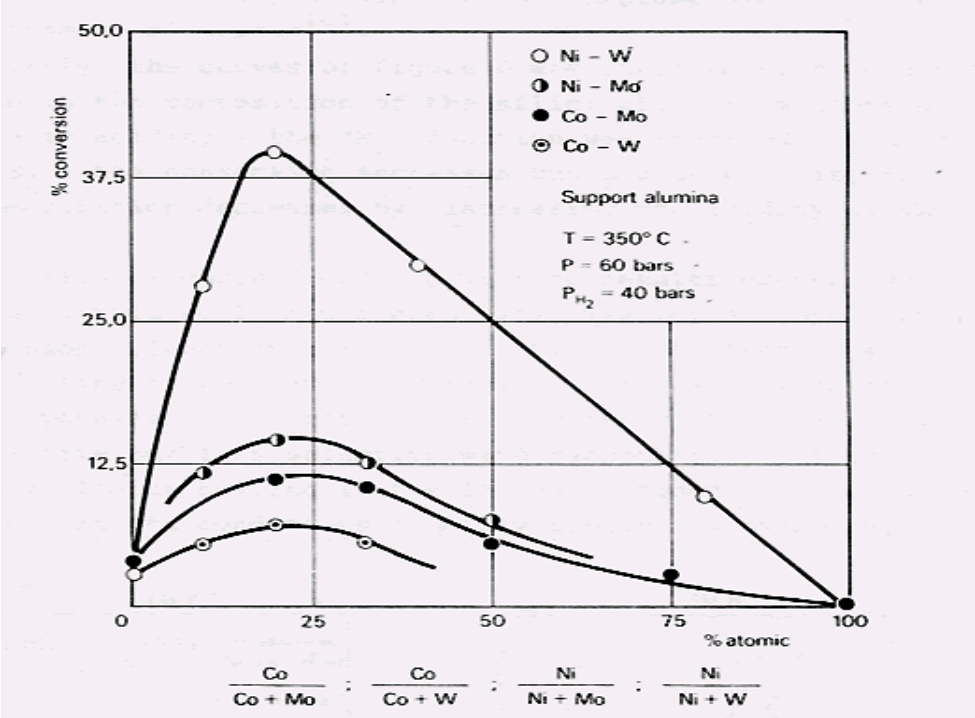


**Figure 2.2 Optimum metal pair's atomic ratio [20]**

Optimization of a hydrocracking process lies extensively on the balance between hydrogenation and cracking functions. An effective hydrocracking catalyst should have its acid and hydrogenation sites close together in order to be able to promote a very fast molecular transfer to avoid side reactions [20].

Gas oil yield from hydrocracking of oil residue has been analyzed and reported to produce large amount of C-4 and C-6 hydrocarbons. Competition for dissolved hydrogen supplied locally was also observed between catalytic and thermal processes at high temperature. In addition, from all indices of performance, Ni-Mo catalyst was reported to be the most active for hydrocracking of residue from Alberta bitumen. Ni-Mo was reported to perform 10% better than Mo-alumina [23. This observation further buttress the point that nickel promoter is a vital catalyst component for gas oil production.

The zeolites supported noble metal catalyst systems have been reported to have adequate resistance to poisoning by sulfur. The reason for this action is that noble metals lose some of their electrons to the acidic sites of the zeolites, thus, become electro-deficient and resistant to sulfur poisoning [24]. Acidic sites in zeolites act as adsorption surface for aromatic compounds which are hydrogenated therein by hydrogen on metal surface [25].

Developing hydrogenation (HYD) and subsequent ring opening (hydrocracking (HYC)) reactions catalysts with high activity has been of interest to many researchers. A system comprising of elements like molybdenum, nickel and phosphorus supported on zeolite-alumina has been reported to be active catalyst for HYD and HYC of alkylated tetralin and PAHs which yielded BTEX (benzene, toluene, ethylbenzene and xylene) [26]. However, a different report confirmed the catalytic cracking of aromatic hydrocarbons to BTX by USY zeolite in the absence of metals [27, 28]. Hydrogenation and hydrocracking of LCO have been investigated using ITQ-2 supported platinum and reported to reduce aromatics compounds to a very low amount. However, USY- zeolite supported platinum has been proved to be better in terms of alkylated benzene products because of its pores and acidity [29, 30]. Similar researches on tetralin and decalin with special attention to different zeolitic porosity were also reported [31].

## 2.2 Mechanism of hydrocracking

Liu and co-workers 2008 [15] reported selective ring opening (SRO) of naphthalene employing $Mo_2C$-HY catalyst but, catalytic activity was declined with increasing amount $Mo_2C$ as it weakens the acid sites which have been implicated in SRO. Figure 2.3 shows

the reaction schemes for catalytic hydrogenation and hydrocracking of naphthalene via monomolecular and bimolecular pathways [31].

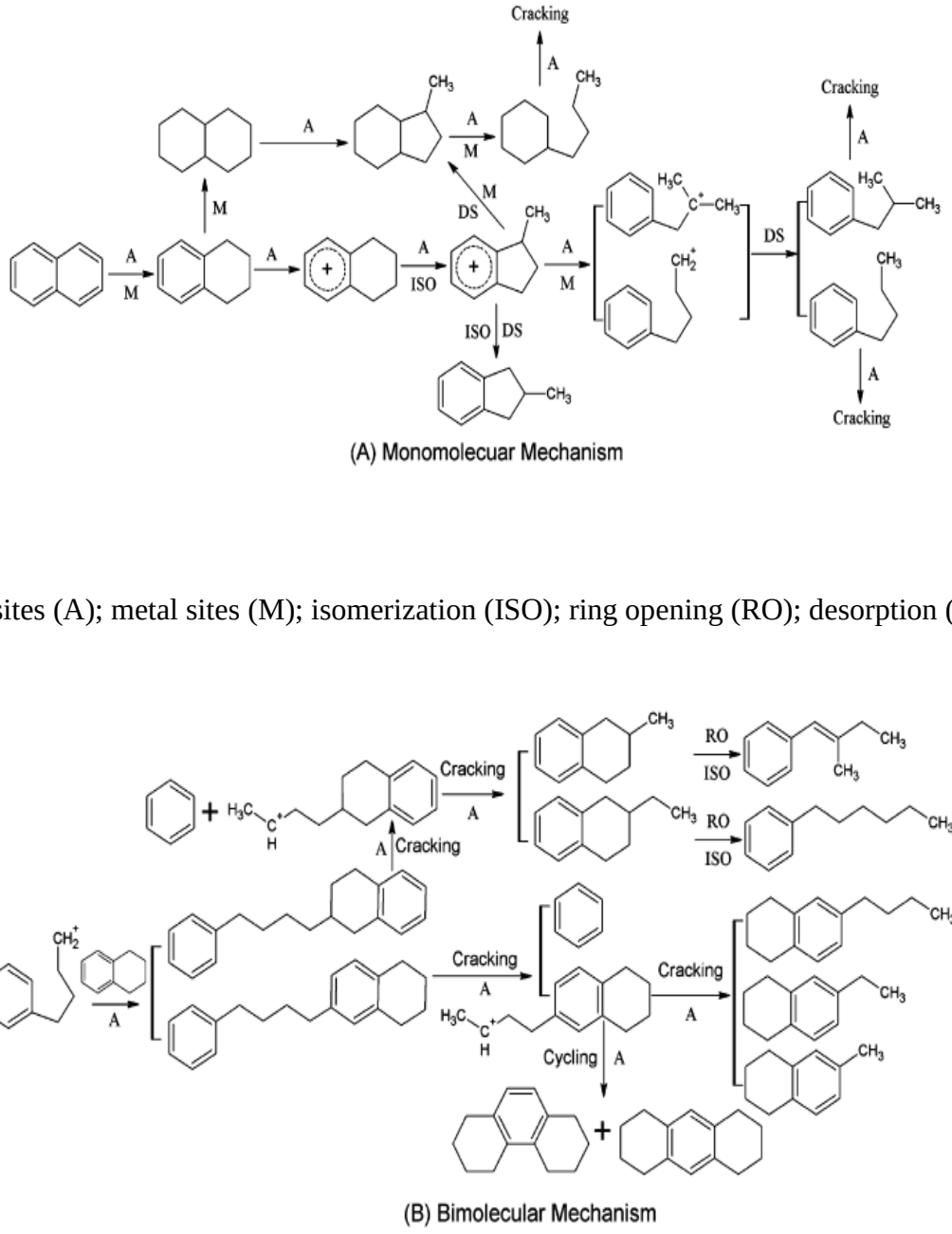


Acid sites (A); metal sites (M); isomerization (ISO); ring opening (RO); desorption (DS)

**Figure 2.3 Monomolecular and bimolecular reaction mechanisms for catalytic hydrogenation and hydrocracking of naphthalene.**

## 2.3 Hydrodesulfurization (HDS) Mechanisms

Mossbauer spectroscopic experiments confirmed cobalt-molybdenum-sulfur (Co-Mo-S) model and it has since been the most accepted model for active phase in hydrodesulphurization [32, 33]. The catalytic active sites (Co-Mo-S) were decorated by atoms of cobalt with stacks of molybdenum sulfide. It is also possible to have cobalt ions attached firmly to the support and grains ($Co_9S_8$). Both grains of $Co_9S_8$ or Co-Mo-S phase is relatively larger on the sulfide catalyst depending on the amount of molybdenum and cobalt and pretreatment carried out [31].

In HDS over sulfide Co-Mo, the mechanism was reported to involve Hydrogenolysis as depicted in figure 2-4 [35]. The mechanism shows a dissociative adsorption of gaseous hydrogen on the surface of the catalyst with replenishment of consumed hydrogen via surface spillover. In a Similar manner, the mechanism of HDS when Mo-MCM-41 was used as catalyst is as shown in figure 1-5. The breaking and formation of bonds occurs between Mo atoms at the edges and their surrounding Mo atoms. A slower rate of HDS was proposed for Mo catalyst than Co promoted Mo catalyst because the Mo-S attached to the Mo atom at the edge is more difficult to cleave than Co-S.

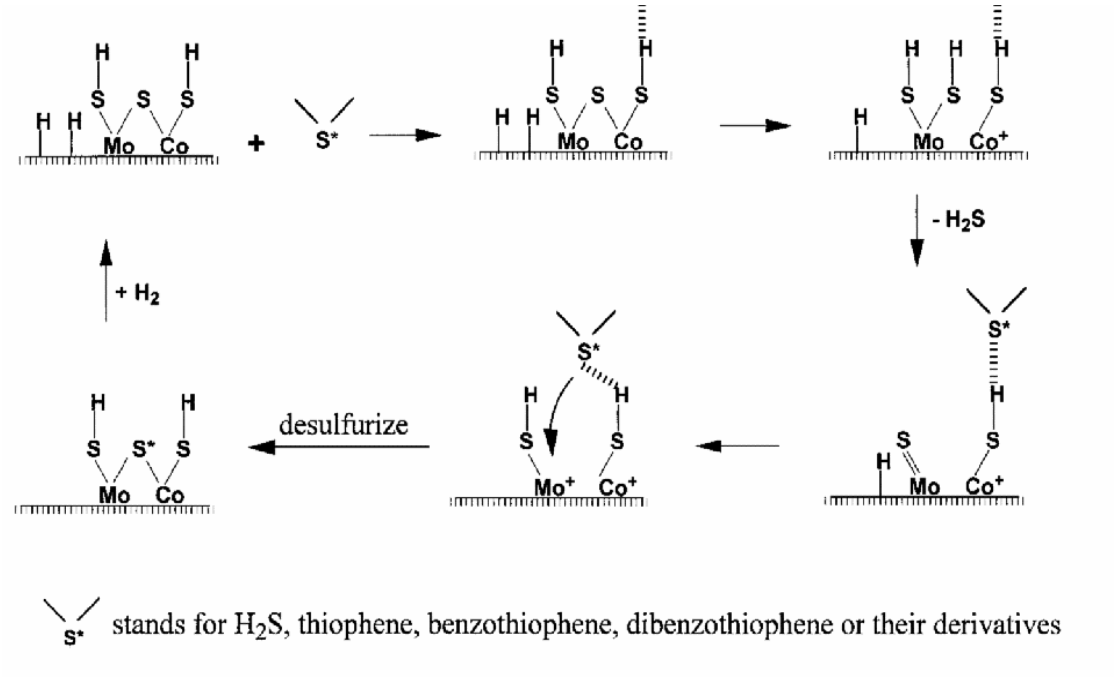


**Figure 2.0.4 Hydro desulfurization mechanism over sulfided Co-Mo catalysts [35]**

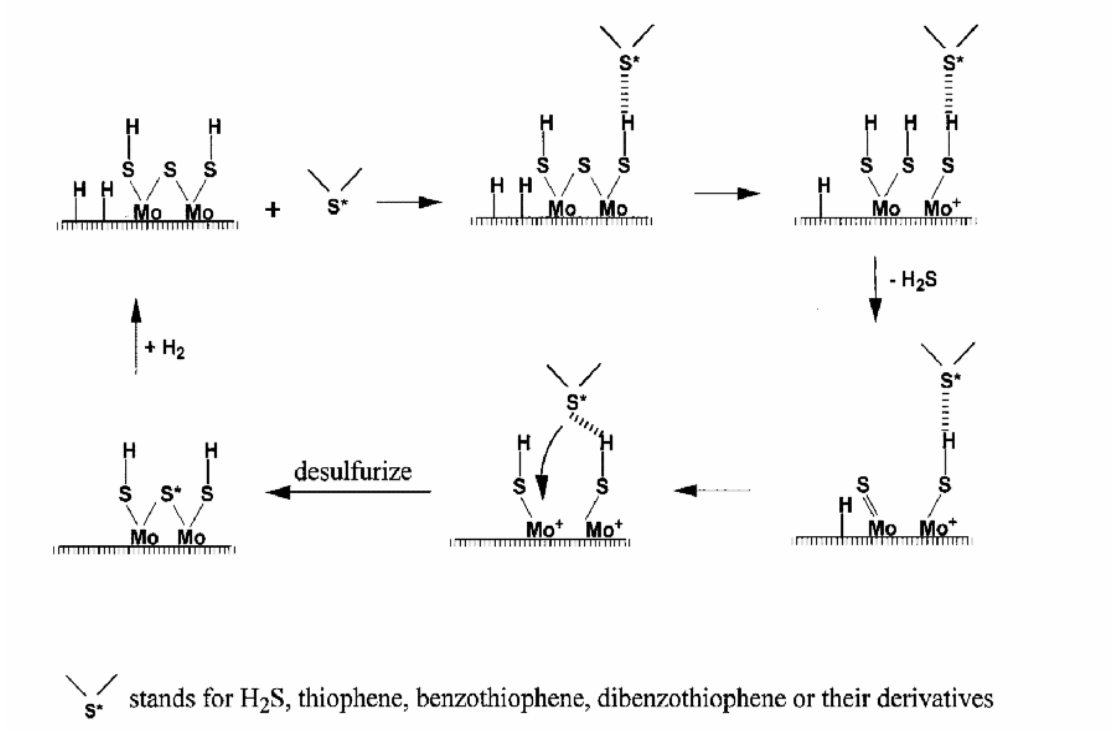


**Figure 2.5 Hydrodesulfurization of mechanism of DBT over sulfided Mo catalysts [35]**

It is now pertinent to conduct a cutting-edge research in order to design a catalyst system, with adequate porosity (mesopores) to accommodate heavy molecules; acidity to suit desired products yield and selectivity and very high hydrogenation efficacy. This is, indeed, the new direction in petroleum refining and particularly hydrocracking.

# CHAPTER 3

# EXPERIMENTALS

## 3.1 Materials

Dodecane (>= 99%, Sigma-Aldrich, Germany), $PdCl_2$, $RuCl_3.3H_2O$ (1.5% in $HNO_3$, Pressure Chemicals, Inc.), Naphthalene crystals (Fischer Scientific Company, USA),boric acid, xylene (Sigma-Aldrich, 99+%, ortho, meta and para), decalin and tetralin (Sigma-Aldrich, 98%), CBV 500 (Zeolyst international; $SiO_2/Al_2O_3$ Mole Ratio: 5.2, Nominal Cation Form: Ammonium, $Na_2O$ Weight %: 0.2,Unit Cell Size, Å: 24.53, Surface Area, $m_2$/g: 750) Y zeolite, $Al_2(SO_4)_3.18H_2O$ (Alfa Aesar), benzene, methylcyclohexane (Fluka AG, 98%), ethylbenzene (Fluka AG, 98%), toluene ((Sigma-Aldrich, 99+%), double deionized water (DDW), Nitric acid, hydrochloric acid, Pd $(NH_3)_4Cl_2.H_2O$ (99.9%) (FW=263.46 g/mol, Alfa Aesar) and Ru $(NH_3)_6Cl_3$ (98%) (FW=309.61, Aldrich).

## 3.2 Preparation of bifunctional hydrocracking catalysts

It is clear that the characteristics which translate to performance of a catalyst is largely dependent on its constituents, preparation method adopted and conditions of preparation such as; molar ratio of reactants used, pH, time, rate of stirring and sequence of adding reactants [8]. Based on critical review of literature, Ruthenium and Palladium are chosen as metals to be incorporated on ultra stable Y-zeolite. The decision was informed

by good hydrogenation ability of these metals and acidity of USY support [14-20]. The as-received Y zeolites was treated as depicted (figure 3.1) and discussed below.

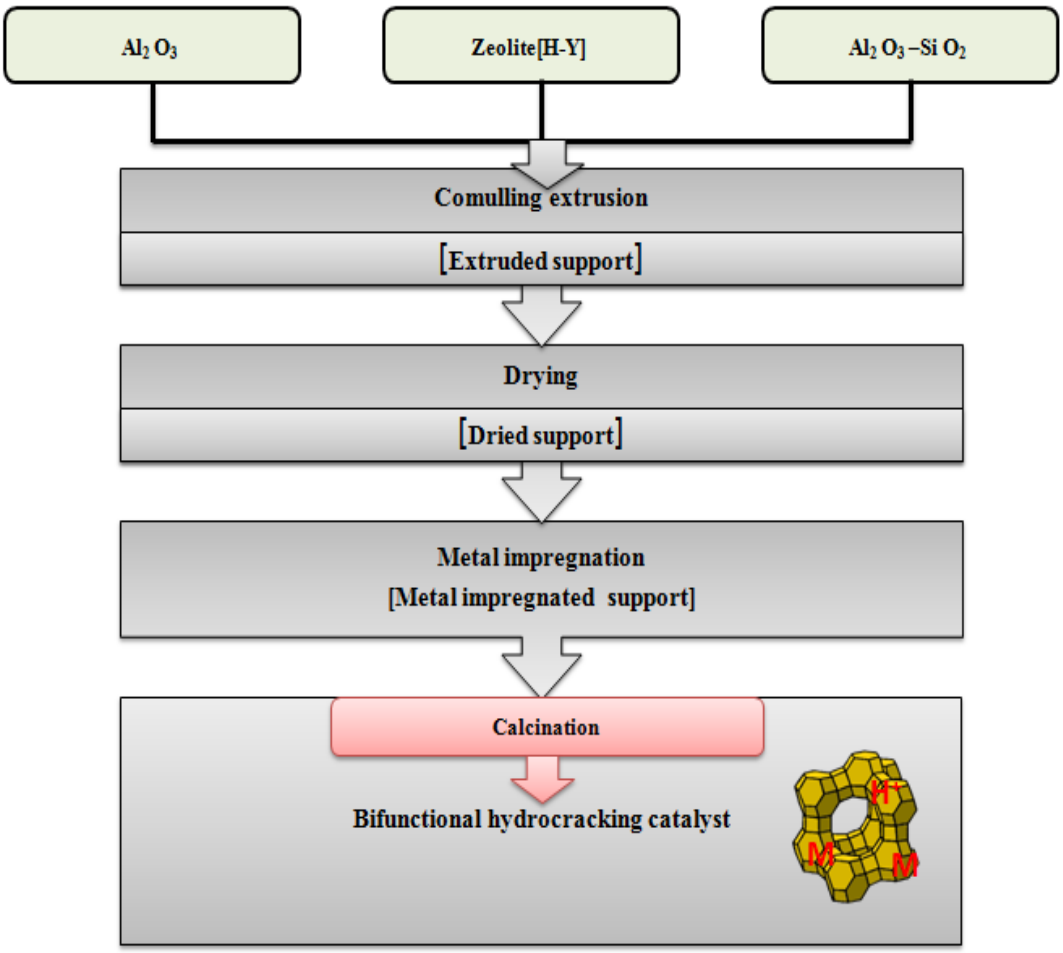


**Figure 3.1 Technique for preparing bifunctional hydrocracking catalyst**

1. **Comulling and Extrusion**: Y-zeolite (acidic) was mixed with alumina binder as required and while other variant of support is without alumina. The mixing was done till they become homogenous. Addition of deionized water to the mixture gave dough which is the form that will undergo extrusion with the aid of a syringe.
2. **Drying:** this is done overnight at a temperature of 85 $^{0}$C extruded catalyst will be dried overnight to exclude any adhering moisture in the catalyst support.
3. **Calcination:** this is a temperature-programmed operation which can be applied both

before and after incorporation of metals. The process eliminates water molecules, organic materials, volatile and unstable ions. This step has a great impact on the physical characteristics (stability, surface area, wear resistance, pore size distribution, etc.) of the catalyst support. In-adequate drying or calcinations process can lead to structural damage of the catalyst (loss crystallinity), damage to active sites, loss of pores, and reduction in surface area. These are critical factors that determine catalytic performance. Calcination procedure is as highlighted below:

1. Temperature is ramped from $25^0$C to $120^0$C at $10^0$C /min heating rate for half an hour.
2. Temperature is ramped from $120^0$C to $250^0$C at 5 $^0$C /min heating rate for half an hour.
3. Temperature is ramped from $250^0$C to $550^0$C at 2 $^0$C /min heating rate for 8 hours.
4. **Impregnation:** this is an operation that introduces metal in to the support. There are various methods for achieving this like, ion exchange, dipping, evaporative impregnation, and incipient wetness impregnation. For this research, ion exchange was employed which is very for preparing hydrocracking catalyst.

### 3.2.1 Ion Exchange

For the ion exchange process for the as-received catalyst, a stock solution of the desired salt(s) was used. The step-by step procedure for this is as follows:

1. Measure solution of the desired ion into a beaker and introduce the zeolite (10-15ml of solution to 1g of zeolite) with continuous and adequate stirring rate.
2. After several hours, filter the sample and oven-dry (or at room temperature) overnight.
3. Carryout calcinations as previously explained.

The step-by-step procedure employed in this research is as detailed below:

Stock solution:

- 20 mM concentration (10 mM $Pd^{+2}$ and 10 mM $Ru^{3+}$)
- Total volume 500 ml
- pH ~ 9 (adjusted using 29% $NH_4OH$)

Prepared by dissolving 1.3186 g Pd $(NH_3)_4Cl_2.H_2O$ (99.9%) (FW=263.46 g/mol, Alfa Aesar) and 1.5796 g Ru $(NH_3)_6Cl_3$ (98%) (FW=309.61, Aldrich) in water in 500 ml volumetric flask with its pH adjusted using $NH_4OH$ to ~9.

**Catalysts:**

1) **RuPdECY B-Series (Y zeolite):**

Zeolite Y in $NH_4^+$ form (Zeolyst CBV-500) calcined at $550^0$C in static air for 8 h (heating rate 2 deg Celsius $min^{-1}$)

**I. RuPdECY-1B: (20mM solution)**

- 10.0 g of Y-zeolite was soaked in 100.0 ml of stock solution
- pH was maintained at ~9 by adding 0.1-0.2 ml $NH_4OH$
- Stirred at room temperature (~22 $^0$C) for ~5 min
- Filtered in 2 min
- Allowed to dry at room temperature for 24 h

**II. RuPdECY-2B: (10 mM solution)**

- 50 ml of 20mM stock solution was used to make 100 ml of 10 mM solution (PH~9)
- Same as for 1B

**III. RuPdECY-3B: (5 mM solution)**

- 25 ml of 20 mM stock solution was used to make 100 ml of 10 mM solution (PH~9)
- Same as for 1B

**IV. RuPdECY-4B: (2.5 mM solution)**

- 12.5 ml of 20 mM stock solution was used to make 100 ml of 10 mM solution (PH~9)
- Same as for 1B

**2) <u>$Al_2O_3$-YD (D) series support</u>**

a) 80 g of Zeolite Y in $NH_4^+$ form (Zeolyst CBV-500) was dispersed in 250 ml of 0.5M (aq) solution of $Al_2(SO_4)_3.18H_2O$ and stirred at room temperature for 100 minutes.

b) The solid was filtered and then dried at 85 $^0$C for 24 h.

c) The dried solid was then washed in 1 M $NH_4OH$ solution then filtered, washed with deionized water, and then dried at 85 $^0$C for 24 h.

d) The solid was calcined at 550 C in static air for 8 h (heating rate 2 deg $min^{-1}$).

I. **RuPd-$Al_2O_3$-YD1: (20 mM solution)**

- 10.0 g of $Al_2O_3$-YD was soaked in 100.0 ml of stock solution
- pH was maintained at ~9 by adding 0.1-0.2 ml NH4OH
- Stirred at room temperature (~22 C) for ~5 min
- Filtered in 3 min
- Allowed to dry at room temperature for 24 h

II. RuPd-$Al_2O_3$-YD2: (10 mM solution)

- 50 ml of 20 mM stock solution was used to make 100 ml of 10 mM solution (PH~9)
- Same as for D1

III. RuPd-$Al_2O_3$-YD3: (5 mM solution)

- 25 ml of 20mM stock solution was used to make 100 ml of 10 mM solution (PH~9)
- Same as for D1

IV. RuPd-$Al_2O_3$-YD4: (2.5 mM solution)

- 12.5 ml of 20 mM stock solution was used to make 100 ml of 10 mM solution (PH~9)
- Same as for D1

## 3.3 Characterization of prepared hydrocracking catalysts

### 3.3.1 X-Ray Diffraction (XRD) Profiles

The different varieties of the catalyst samples including the supports were subjected to powdered X-ray diffraction measurement in order to confirm their crystallinity nature. High- angle powder X-ray diffraction patterns were recorded on a Rigaku Miniflex II XRD powder diffraction system using CuKα radiation ($\lambda_{K\alpha1}$ = 1.54051Å, 30 KV and 15 mA). The XRD patterns were recorded in the static scanning mode from 5.0 - 60° (2θ) at a detector angular speed of 2 °/min and step size of 0.02°.

### 3.3.2 Inductively-Coupled Plasma Optical Electron Spectroscopy (ICP-OES)

The concentrations of metallic constituents (Si, Al, Ru and Pd) of the catalysts were quantified with the aid of inductively coupled plasma optical emission spectroscopy (ICP-OES) on a Spectro Ciros Vision (FV E12) instrument. The digestion of the samples was carried out using aqua regia and hydrofluoric acid (HF) which is known to dissolve silicon in order to be able to measure it quantitatively with high level of accuracy.

The digestion procedure is as illustrated below [36]:

1. Weigh 0.5g of the catalyst into 50ml rubber container with a tight cover.
2. Add 4ml of freshly prepared aqua regia (3ml HCl: 1 ml $HNO_3$). The two solutions can be added one after the other to minimize the effervescence.
3. Add 3ml of hydrofluoric acid cover tightly and shake very well.
4. Heat the samples to 80-95 $^0$C on a heating block in a working fume hood for 4 to 6 hours.
5. Remove the sample and allow cooling.
6. Add about 4g of boric acid to trap the HF. This is needed in excess to avoid losing part of the silicon in the form $SiHF_3$.
7. Make up the volume to mark using 1-2% $HNO_3$
8. Filter the sample and the filtrate is ready for analysis.

### 3.3.3 Surface Area Measurement

Textural properties were characterized by $N_2$ adsorption-desorption measurements at -196 $^0$C, with the aid of Micromeritics ASAP-2020 adsorption analyzer. Outgassing of the

catalyst samples was carried out in vacuum of $10^{-5}$ torr at a temperature of 220 $^0$C for 180 minutes before $N_2$ physi-sorption. The adsorption data were utilized in the range of 0.06 to 0.30 ( relative pressure ($P/P_0$) in accordance with the Brunauer-Emmett-Teller (BET) for specific surface area determination with the assumption of cross-sectional area of 0.164 $nm^2$ for $N_2$ molecule. From Lippens and de Boer approach [37], *t*-plot was used to evaluate the contribution of micro- and meso pores. Whereas, the mesopore size distribution was calculated using the Barret-Joyner-Halenda (BJH) pore size model applied to the adsorption branch of the isotherm [38]. With Kelvin's equation and the assumption that the pore geometry is cylindrical, mesopore size can be calculated from the equation below:

$$r_k = \frac{-2\gamma Vm}{RTln\left(P/P_0\right)}$$

Where $\gamma$ is the surface tension of nitrogen at its boiling point (8.85 ergs/$cm^2$ at 77K).

$Vm$ = molar volume of liquid nitrogen (34.65$cm^3$/mol).

$R$ = gas constant (8.314x$10^7$ergs/deg mol).

$T$ = boiling point of nitrogen.

$P/P0$ = relative pressure of nitrogen.

$rk$ =the Kelvin radius of the pore.

The pore radius which is referred to as Kelvin radius (rK) corresponds to the radius at which condensation is observed vis-à-vis the relative pressure ($P/P_0$. However, before

condensation starts, there is adsorption on the surface of the pores which will make rk less of the actual pore radius. Therefore, the thickness of the adsorbed layer before condensation (t) should be added to the value or rk to get the actual pore radius. The equation given below results;

$$r_p = r_K + t$$

t = the thickness of the adsorbed layer. t is given by: $t(A^0) = 3.54\left[\frac{5}{2.303log\left(P_0/P\right)}\right]^{1/3}$

Total pore volume is derived from the amount of vapor adsorbed at a relative pressure by assuming that pores are filled with liquid adsorbate. From the linearized equation of Braunauer, Emmett and Teller written below, the surface area of the material can be derived.

$$\frac{P}{V_a(P_0 - P)} = \frac{1}{V_m C} + \frac{c-1}{V_m C}\left(\frac{P}{P_0}\right)$$

$V_a$ = amount of gas adsorbed corresponding to relative pressure ($P/P_{0)}$

$V_m$ = amount of adsorbate corresponding to a single layer coverage.

C is Braunauer, Emmett, Teller constant which indicates amount of energy involved in adsorption for the first single layer. It also reveals information about the interactions between the adsorbent and the material adsorbed on to the surface. This approach measures the amount of nitrogen adsorbed at $-196^0$C boiling point against different values of pressure (partial) which should below 1 atm. Finally, the amount of adsorbed gas in volume unit is determined by measuring the change in pressure for a known amount of $N_2$ gas over a sample.

### 3.3.4 Scanning Electron Microscopy (SEM)

Scanning Electron Microscopy (SEM) was performed on prepared catalysts to determine the particle size and morphology. The SEM images were recorded using FESEM/FIB (Tescan Lyra-3). The field Emission Dual Beam (Electron/ Focused Ion Beam) system combines high-end field-emission scanning electron microscope (FESEM) and high-performance focused ion beam (FIB) system in one chamber.

### 3.3.5 Transmission Electron Microscopy (TEM)

Field Emission Transmission Electron Microscopy (FETEM) was used to capture the images using a JEOL JEM-2100 FX microscope which was operated at 80 KV ( 200Kv for STEM) and equipped with a charge coupled device camera (Gatan).Prior to the characterization, samples were sonicated in ethanol to properly dispersed its constituents. The resulted suspensions were deposited on a micro-grid with carbon supported on a 300 mesh copper grid of diameter 3.0mm.

### 3.3.6 Temperature Programmed Reduction (TPR)

TPR is used to monitor metal support interactions. It also provides useful information about the temperatures needed for the complete reduction of a catalyst. For bimetallic catalysts, TPR patterns often indicate whether two components are mixed or not. Reduction is an inevitable step in the preparation of metallic catalysts. The reduction of metal oxide $MO_n$ by $H_2$ is described by the equation.

$$MO_n + nH_2 \longrightarrow M + n\,H_2O$$

Reaction of metal oxides with hydrogen starts with dissociative adsorption of $H_2$, which is a much more difficult process on oxides than on metals. Rate expression for the reduction reaction under conditions where the reverse reaction from metal to oxide can be ignored is:

$$-d\frac{[MO_n]}{dt} = k_{red}[H_2]^p f([MO_n])$$

Where: $[MO_n]$ is the concentration of metal oxide

$[H_2]$ is the concentration of hydrogen gas.

$k_{red}$ is the reduction constant.

*P* is the order of reaction with respect to hydrogen gas.

*F* is the rate dependent function on metal oxide.

t is the time.

Temperature programmed reduction ($H_2$-TPR) was carried out using Micromeritics AutoChem II 2920VGCR. Samples of 0.2 g were heated under hydrogen flow (50 $cm^3$/min; 10 % $H_2$ in Ar) from room temperature to 673 k at a rate of 5 k $min^{-1}$. Chemisorptions were carried out on the reduced samples using 10% $H_2$ in Ar in order to determine total hydrogen up-take by the supported metal. Ammonia Temperature programmed desorption ($NH_3$-TPD) was done using the same instrument after drying the reduced samples at 673 k under the flow of Nitrogen.

## 3.4 Catalytic Evaluation

### 3.4.1 Batch Autoclave Reactor

A batch autoclave reactor (Parr pressure reactor, 300 ml working volume) is identified as appropriate for monitoring high exothermic hydrocracking reactions. It can withstand constant temperature reaction over reasonable period of time, proper fluid contact and very easy to operate. It aids determination of both activation energy and intrinsic reaction order.

The reactor is fitted with a stirrer and housed in an electronic furnace. There is programmed control system for setting temperature of reaction, speed of the stirrer. Pressure and flows is controlled manually. Chiller is connected to keep the temperature of the pressure monitoring panel to the barest minimum as excessive temperature from the exothermic reaction can damage it.

This work is designed to hydrogenate and crack naphthalene to lower molecular weight hydrocarbons using very little amount of catalysts. The reaction parameters are the same for all the variants of catalysts tested as listed in the table 3.1

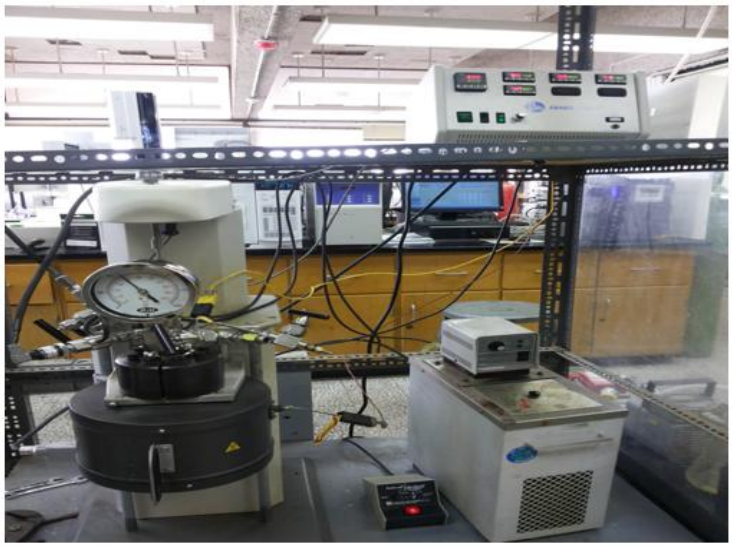

**Figure 3.2 An autoclave batch reactor**

**Table 3.1 Reaction parameters**

| Parameter | RuPdECY-B | RuPd-$Al_2O_3$-YD |
|---|---|---|
| **Feed(wt% ) | 10 | 10 |
| Volume of feed (ml) | 100 | 100 |
| Catalyst amount (g) | 0.25 | 0.25 |
| Pressure (bar) | 50 @ 25 $^0$C | 50 @ 25 $^0$C |
| Temperature ($^0$C) | 300 | 300 |
| Stirring rate (rpm) | 300 | 300 |

**naphthalene dissolved in dodecane

### Batch Reaction Procedure

100 ml of the prepared feed (10 wt %) which was done by dissolving 100g of naphthalene in 1litre of pure dodecane was fed into the reactor. The required weight of previously reduced catalyst (reduction in furnace from 25 $^0$C at 10 $^0$C/ min 400 $^0$C under continuous flow of hydrogen (70 $cm^3$ $m^{-1}$) for 2 hours) was charged into the reaction vessel. Both $H_2$ and $N_2$ were used at different point to check for leak. The temperature was allowed to rise gradually to reaction temperature of 300 $^0$C. Samples were collected at interval of 30 minutes for 4 hours with sample collected at 300 $^0$C representing product at time zero. All collected samples were analyzed offline using gas chromatography fitted with flame emission detector (GC-FID).

### Gas Chromatography Analysis (GC-FID)

The quantitative analysis of different samples collected was done using GC-FID (Agilent technologies 7890A. Prior to feeding the samples into the GC, the system was calibrated using known concentrations of expected products. Further confirmation on retention times was established was using Gas chromatography Mass Spectrometry (GC-MS) fitted with column of the same specifications. The detailed of the GC parameters are as listed below:

**Figure 3.3 Gas chromatograph flame ionization detector (GC-FID) set-up**

**GC-FID**

Inlet volume (µl) 1

Inlet mode: Split

Split ratio 5: 1

Inlet temp. ($^0$C) 280

Inlet pressure (psi) 11.3

Oven temp. ($^0$C) 35–100 $^0$C (1 $^0$C/min)–125 $^0$C (1 $^0$C/min)–200 $^0$C (10 $^0$C/min)

Air (psi) 400

**GC-MS** Inlet volume (µl) 3

Inlet mode = Split (5:1)

Inlet temp. ($^0$C) 280

Inlet pressure (psi) 11.3

Oven temp. 35–100 $^0$C (1 $^0$C/min)–125 $^0$C (1 $^0$C/min)–200 $^0$C (10 $^0$C/min)

The same DB-1 column (30m x 320µm x 1µm) was used in GC-FID and GC-MS.

# CHAPTER 4

# RESULTS AND DISCUSSION

## 4.1 Metal compositions of the catalysts

In order to confirm quantitatively and adequately obtain the metal loading of the series of catalysts prepared, inductively-coupled plasma optical electron spectroscopy (ICP-OES) was used. The chemical analysis of metal ions requires sample pretreatment to separate the target analytes from the interfering matrix which was done by digesting the samples in acid solutions ($HNO_3$, HCl and HF) and pre-concentrate to the analytical measurable amounts [31,36]. This was done using the method described in section 3.3.2

The results revealed the amount of metals (Al, Si, Ru and Pd) with more aluminium in Alumina-coated support than naked Y zeolite as expected. The amount of Pd in all catalysts is more than Ru with their sum ranging from 1.51 wt% to 0.16% for B-series and 1.08 wt% to 0.20 wt% in D-series. The various obtained loadings and ratios are listed in tables 4.1-3.The single-metal loading Ru and Pd as shown in table 4.1 is around 0.5 wt. % and the amount of Si is approximately half of Al with the Al content in Ru-$Al_2O_3$_YD and Pd-$Al_2O_3$_YD slightly higher than what was observed for RuECY-B and PdECY-B. The extra Al for the D-series was from the alumina used in coating the D-series support. For the same reason and as shown in table 4.2 and 4.3, Al content of D-series bimetallic catalysts was also observed to be more than those in B-series. The more Al content is expected to translate to less acidic behavior of the support.

**Table 4.1 Metal loading of prepared single metal supported ECYB and $Al_2O_3$_YD catalysts by ICP-OES**

| Catalyst | Si (wt. %) | Al (wt. %) | Si+Al (wt. %) | Si/Al | Ru (wt. %) | Pd (wt. %) | Ru_Pd (wt. %) |
|---|---|---|---|---|---|---|---|
| RuECY-B | 4.95 | 9.23 | 14.18 | 0.54 | 0.44 | - | - |
| PdECY-B | 4.45 | 8.35 | 12.80 | 0.53 | - | 0.50 | - |
| Ru-$Al_2O_3$_YD | 4.87 | 10.08 | 14.95 | 0.48 | 0.48 | - | - |
| Pd-$Al_2O_3$_YD | 5.30 | 10.11 | 15.40 | 0.52 | - | 0.51 | - |

**Table 4.2 Metal loading of prepared bimetallic RuPdECYB catalysts by ICP-OES**

| Catalyst | Si (wt. %) | Al (wt. %) | Si+Al (wt. %) | Si/Al | Ru (wt. %) | Pd (wt. %) | Ru_Pd (wt. %) |
|---|---|---|---|---|---|---|---|
| RuPdECY-1B | 15.64 | 9.44 | 25.08 | 1.59 | 0.59 | 0.91 | 1.51 |
| RuPdECY-2B | 15.42 | 8.77 | 24.19 | 1.69 | 0.26 | 0.42 | 0.68 |
| RuPdECY-3B | 15.71 | 9.23 | 24.94 | 1.63 | 0.14 | 0.18 | 0.32 |
| RuPdECY-4B | 15.90 | 8.80 | 24.70 | 1.73 | 0.05 | 0.11 | 0.16 |

**Table 4.3. Metal loading of prepared bimetallic RuPd-$Al_2O_3$-YD catalysts by ICP-OES**

| Catalyst | Si (wt. %) | Al (wt. %) | Si+Al(wt. %) | Si/Al | Ru (wt. %) | Pd (wt. %) | Ru_Pd (wt. %) |
|---|---|---|---|---|---|---|---|
| RuPd-$Al_2O_3$_YD1 | 8.12 | 8.61 | 16.73 | 0.91 | 0.39 | 0.69 | 1.08 |
| RuPd-$Al_2O_3$_YD2 | 8.63 | 9.14 | 17.78 | 0.91 | 0.31 | 0.41 | 0.72 |
| RuPd-$Al_2O_3$_YD3 | 9.67 | 10.31 | 19.99 | 0.90 | 0.24 | 0.26 | 0.50 |
| RuPd-$Al_2O_3$_YD4 | 9.65 | 10.43 | 20.08 | 0.89 | 0.09 | 0.11 | 0.20 |

## 4.2 Temperature Programmed Reduction

Temperature-programmed reduction technique provides qualitative information about the reducibility of metals ion-exchanged into zeolite frame-work. It also gives an insight about what temperature is suitable for reaction. TPR has been widely used for the investigation and characterization of metal incorporated and metal supported catalysts. TPR peak area represents the amount of hydrogen consumption and peak temperature represents the reducibility of the metal oxide or oxides. Thus, TPR results can therefore be interpreted quantitatively as estimates of the distribution of various metal oxide phases as well as the metal support interaction for supported metal oxide catalysts [42].

The concentration of the hydrogen uptake by the catalysts is indicated by thermal conductivity detector (TCD) [43]. The TPR profiles of representative prepared catalysts are as shown in Figures 4.1. There is a clear variation in the peak temperatures which can be attributed to the different metals loaded (Ruthenium and Palladium) and nature of metal-support interactions (naked and alumina-coated zeolite supports) of the catalysts [35]. The metal-support interaction is lower in the alumina-coated zeolite support which contributed to the lower temperature reduction of the metals in D-series catalysts (Pd-$Al_2O_3$_YD and RuPd-$Al_2O_3$_YD2) than those of the B-series (PdECY-B and RuPdECY-2B). The bimetallic catalyst RuPdECY-2B reduced at a temperature in-between the single metal catalysts Ru-$Al_2O_3$_YD and PdECY-B [43]. A very interesting observation was that for every single metal, a characteristic single peak was detected by TCD and even for the bimetallic which is an indication of a proper alloy formation

between Ru and Pd. All the catalyst reduced at less than 300 $^0$C and this informed the decision to carry out the hydrocracking reaction for all the prepared catalysts at 300 $^0$C.

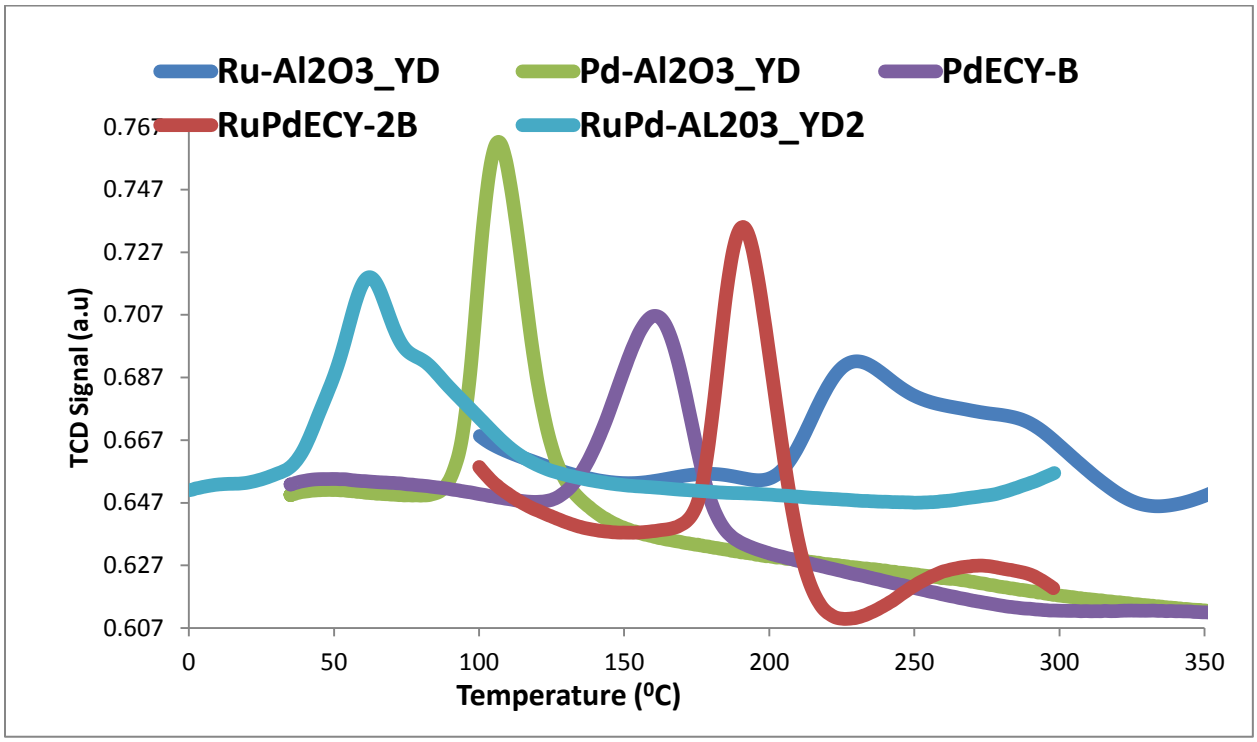


**Figure 4.1 Temperature-programmed reduction of some prepared catalysts**

## 4.3 $H_2$- Chemisorption

Catalyst exists, in most time, as a collection of metal atoms distributed over different support materials such as zeolite and alumina. At the atomic level, it is normal that these atoms are assembled into island-like crystallites on the surface of the support. In the case of supported metal catalysts, it is important to know what fraction of the active metal atoms is exposed and available to catalyze a surface reaction. Those atoms that are located inside metal particles do not participate in surface reactions, and are

therefore wasted. Since these islands vary in size due to both the intrinsic nature of the metal and the support beneath, plus the method of manufacture more or less of the metal atoms in the whole sample are actually exposed at the surface. It is evident therefore that the method of gas adsorption is perfectly suited to the determination of exposed active sites.

Dispersion is defined as the percentage of all metal atoms in the sample that are exposed. The total amount of metal in the sample is termed the loading which forms a percentage of the total sample mass, and is known from chemical analysis like ICP-OES which was used in this research. In the case of the uncoated zeolite catalysts, the effect of metal loading is very clear as the amount of hydrogen gas uptake increases with decreasing loading as shown in table 4.4. This can be attributed to lower dispersion of metal atoms in the RuPdECY-1B (1.51 Wt %) which has the highest metal loading in the B-series catalysts compared to RuPdECY-4B (0.16 Wt %) with lowest metal loading as shown in table 4.2. However, the same trend was not observed for the D-series catalysts (RuPd-$Al_2O_3$_YD1, RuPd-$Al_2O_3$_YD2, RuPd-$Al_2O_3$_YD3 and RuPd-$Al_2O_3$_YD4) . And, in fact, there is no clear effect of metal loading because the coating of the zeolite support reduced to a great extent the metal-support interaction. All the prepared catalysts, regardless of the nature of the supports and metal loading, up-took hydrogen at < 300 $^0$C.

**Table 4.4 Amount of hydrogen uptake by the prepared catalysts with their respective temperature**

| Catalyst | Temperature ($^0$C) | Chemisorptions, $H_2$ µmol/g metal |
|---|---|---|
| RuPdECY-1B | 195 | 19.495 |
| RuPdECY-2B | 196 | 31.453 |
| RuPdECY-3B | 204 | 42.036 |
| RuPdECY-4B | 212 | 50.25 |
| RuECY-B | 246.4 | 7.068 |
| PdECY-B | 161.9 | 8.426 |
| RuPd-$Al_2O_3$_YD1 | 70 | 35.09 |
| RuPd-$Al_2O_3$_YD2 | 66 | 36.365 |
| RuPd-$Al_2O_3$_YD3 | 69 | 39.583 |
| RuPd-$Al_2O_3$_YD4 | 79 | 44.056 |
| Ru-$Al_2O_3$_YD | 229.1 | 10.789 |
| Pd-$Al_2O_3$_YD | 106.8 | 4.478 |

## 4.4 Surface Morphology of Catalysts

In order to confirm the morphologies of the zeolite supports, the prepared catalyst were subjected to electron microscopy analyses. The SEM images revealed the unique octahedral morphology of the Y-zeolite used in this study as shown in the figures 4.2, 4.4, 4.6 and 4.8. The morphology is visible with some particles that can be assumed to be the Ru and Pd ion-exchanged in the framework. No rugged surfaces or cracks were

observed [14, 15]. The observed SEM images have their dimensions ranging between 450 nm and 640 nm.

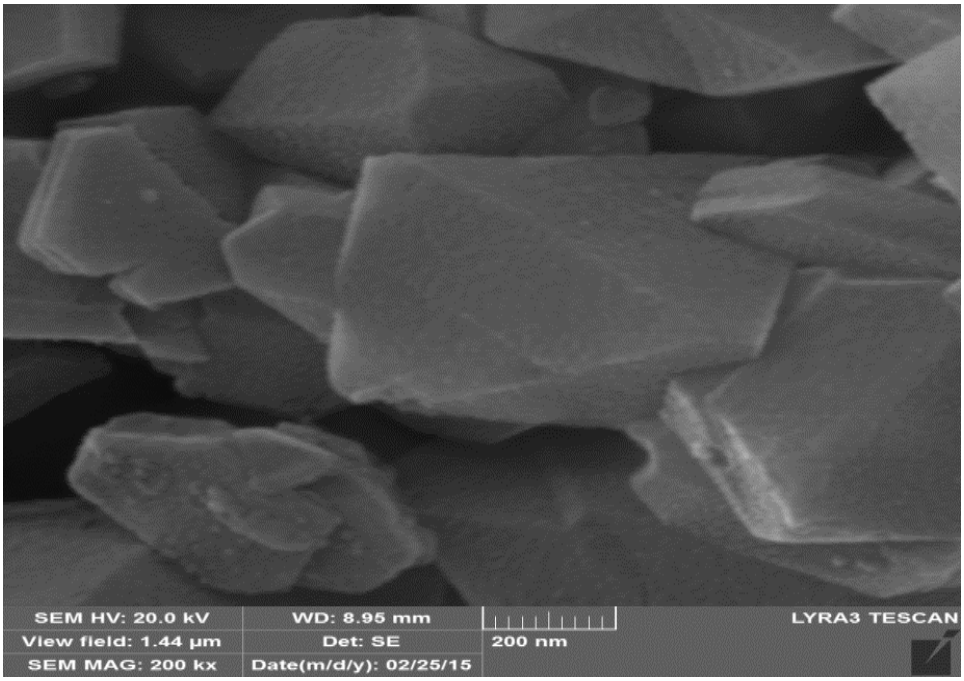


**Figure 4.2 Field Emission Scanning Electron Micrograph of 1.51 wt% RuPdECY-1B.**

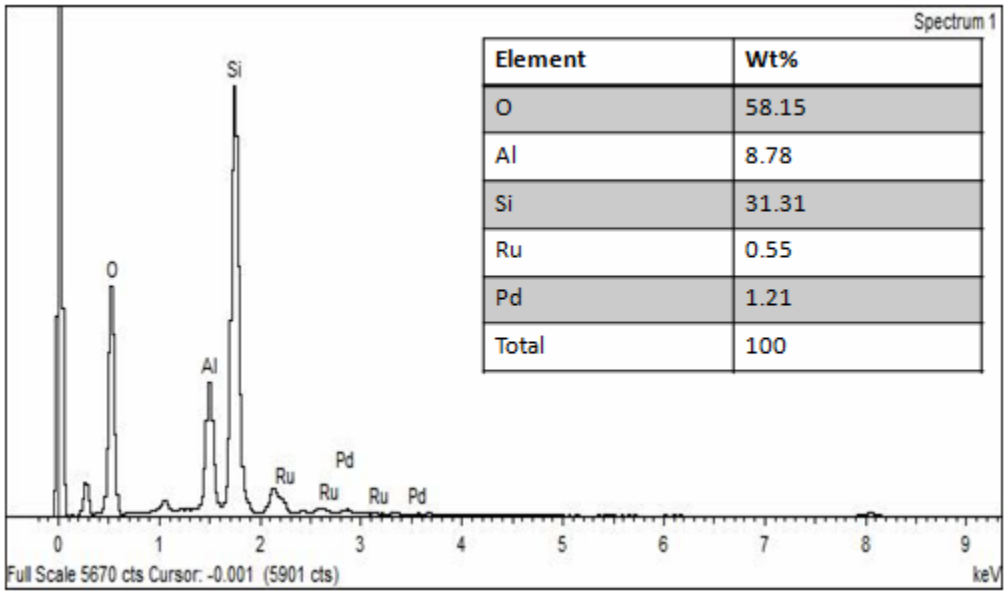


| Element | Wt% |
|---|---|
| O | 58.15 |
| Al | 8.78 |
| Si | 31.31 |
| Ru | 0.55 |
| Pd | 1.21 |
| Total | 100 |

**Figure 4.3 Energy-Dispersive Spectra and elemental composition of 1.51 wt% RuPdECY-1B**

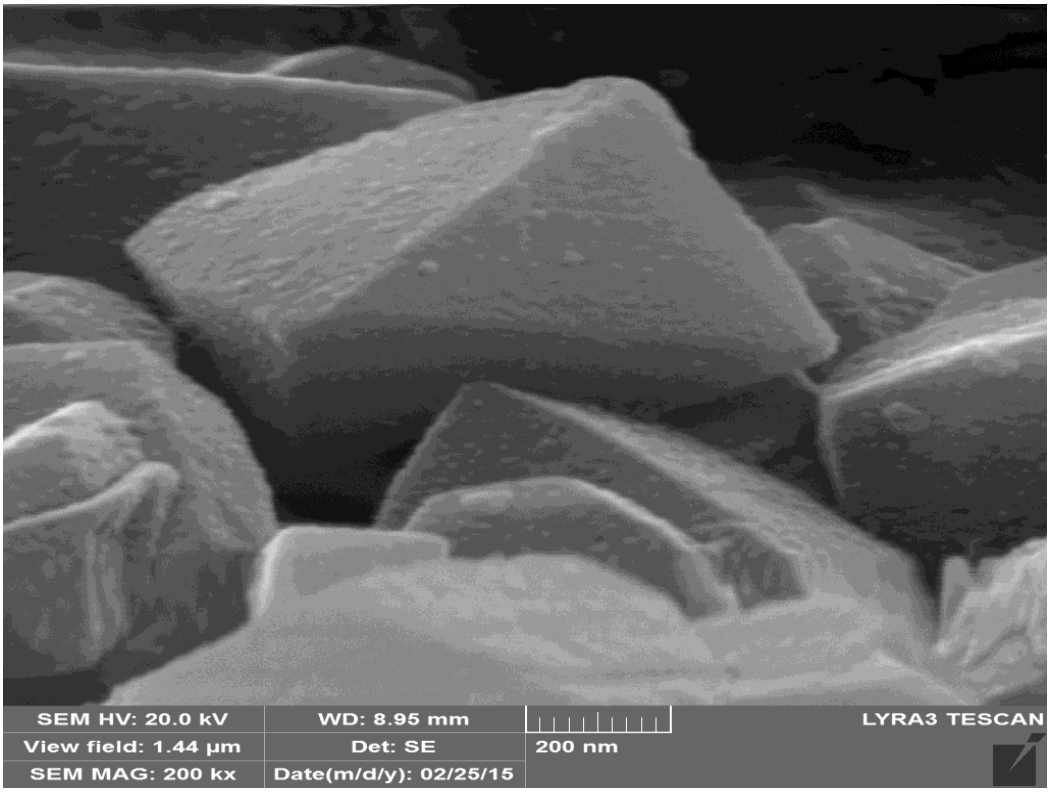


**Figure 4.4 Field Emission Scanning Electron Micrograph of 0.68 wt% RuPdECY-2B.**

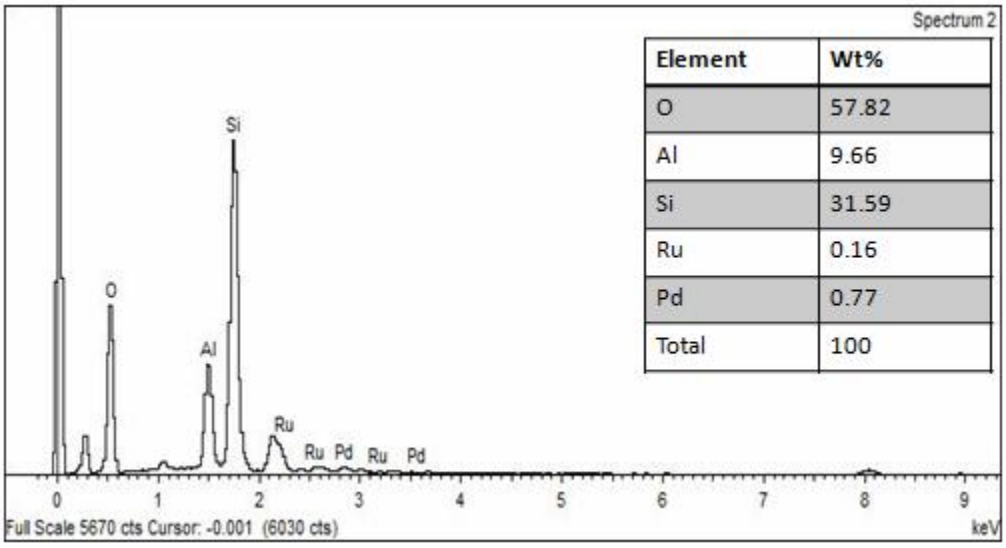


**Figure 4.5 Energy-Dispersive Spectra and elemental composition of 0.68 wt% RuPdECY-2B**

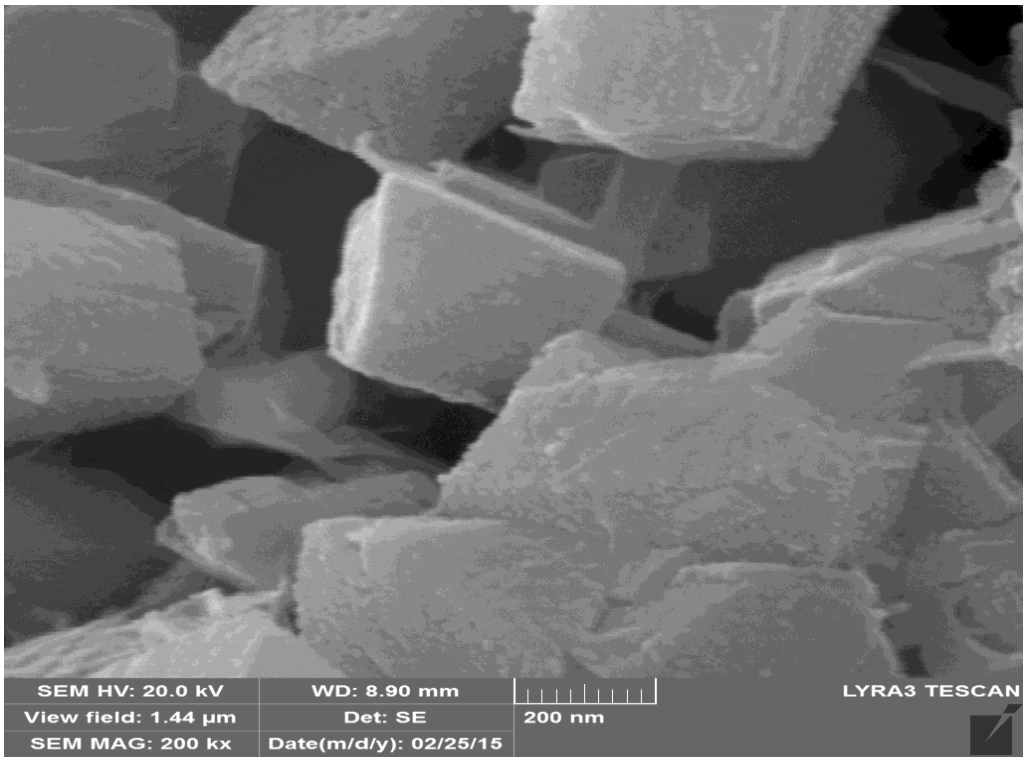


**Figure 4.6 Field Emission Scanning Electron Micrograph of 0.32 wt% RuPdECY-3B**

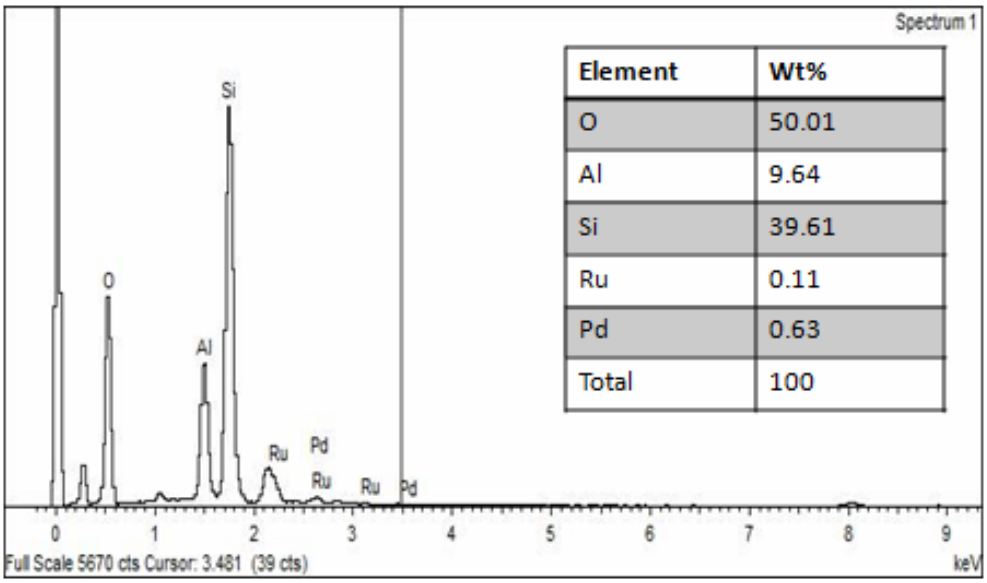


| Element | Wt% |
|---|---|
| O | 50.01 |
| Al | 9.64 |
| Si | 39.61 |
| Ru | 0.11 |
| Pd | 0.63 |
| Total | 100 |

**Figure 4.7 Energy-Dispersive Spectra and elemental composition of 0.32 wt% RuPdECY-3B.**

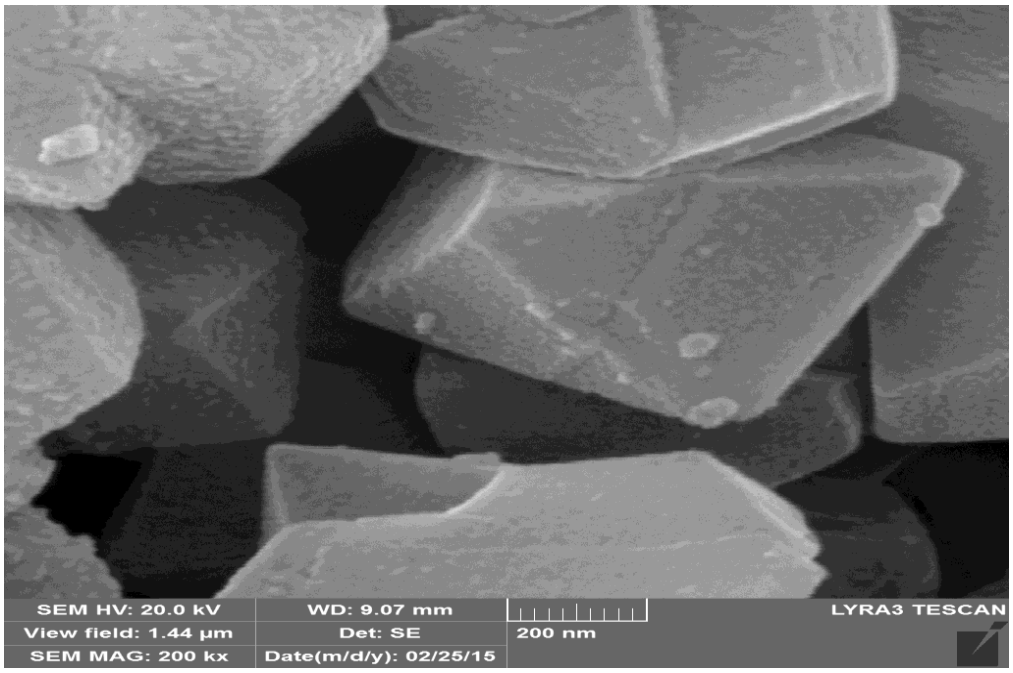


**Figure 4.8Field Emission Scanning Electron Micrograph of 0.16 wt% RuPdECY-4B.**

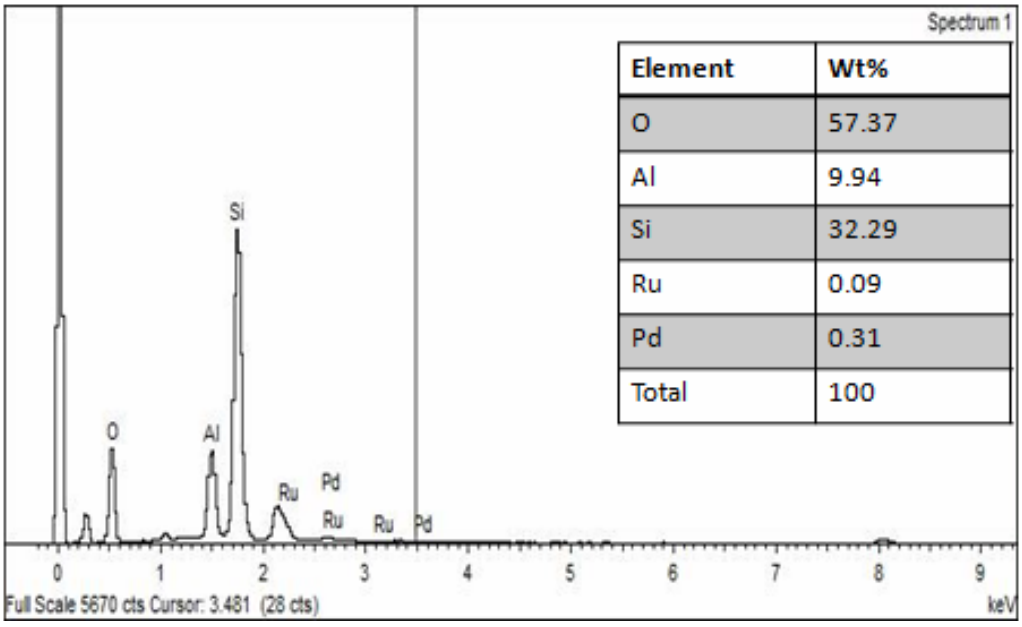


**Figure 4.9 Energy-Dispersive Spectra and elemental composition of 0.16 wt% RuPdECY-4B**

The qualitative analysis of the particles was carried out using energy-dispersive X-ray spectrometry to identify the metals in the supports. The various identified elemental contents of the catalysts are as depicted in figures 4.3, 4.5, 4.7 and 4.9 showing EDS

spectra of respective catalysts. The spectra showed highest intensity for Si among other metals in all the catalysts followed by Al and very low intensities for Ru and Pd confirming their very low amount in the catalysts as expected.

The TEM images are representatives of RuPdECYB and RuPd-$Al_2O_3$-YD catalysts with different amount of metal loading as shown in figures 4.10-17. The images show clearly the excellent distribution of metals (Ru and Pd) on the zeolitic support which is confirmed by Energy-Dispersive spectrometer (EDS). The metal loading difference were clearly observed from the TEM micrographs with the number of meta spots most sparsely dispersed on the catalyst with lowest metal loading.

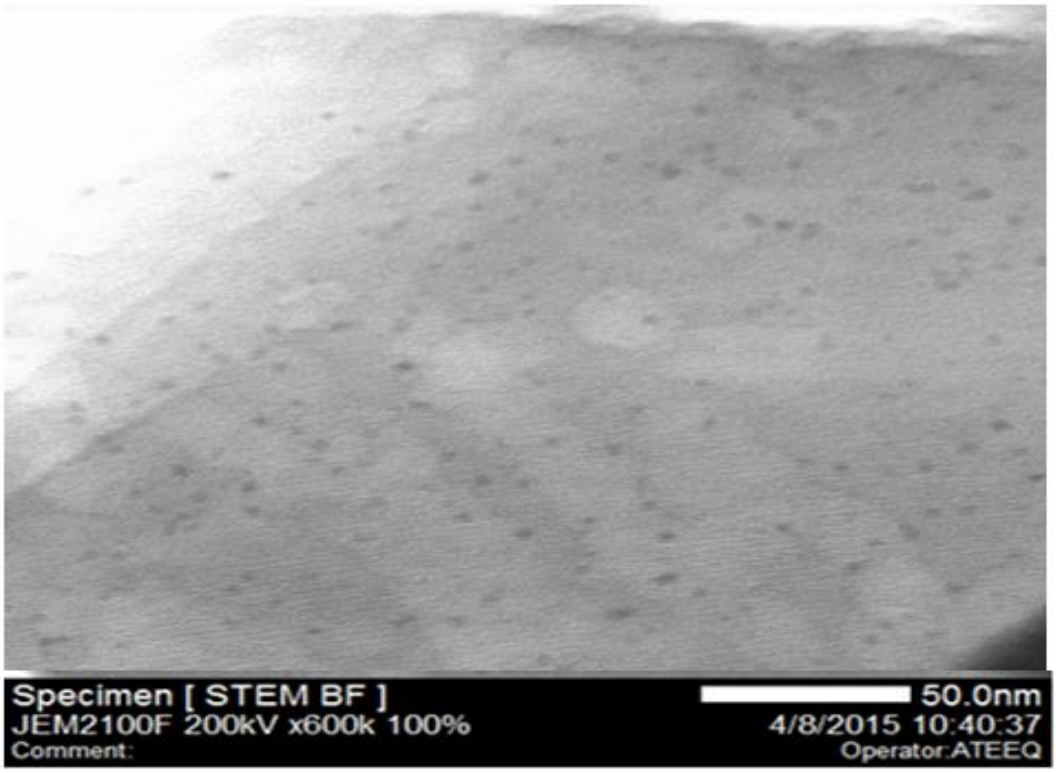


**Figure 4.10 Scanning Transmission Electron Micrograph for 1.51 wt% RuPdECY-1B .**

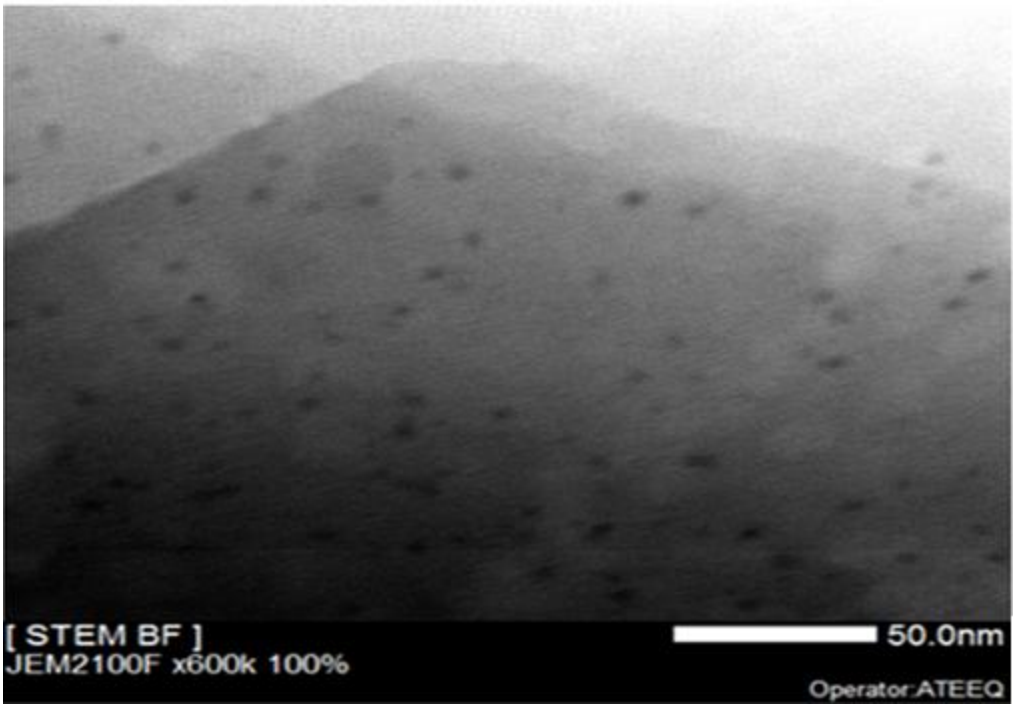


**Figure 4.2 Scanning Transmission Electron Micrograph for 0.68 wt. % RuPdECY-2B**

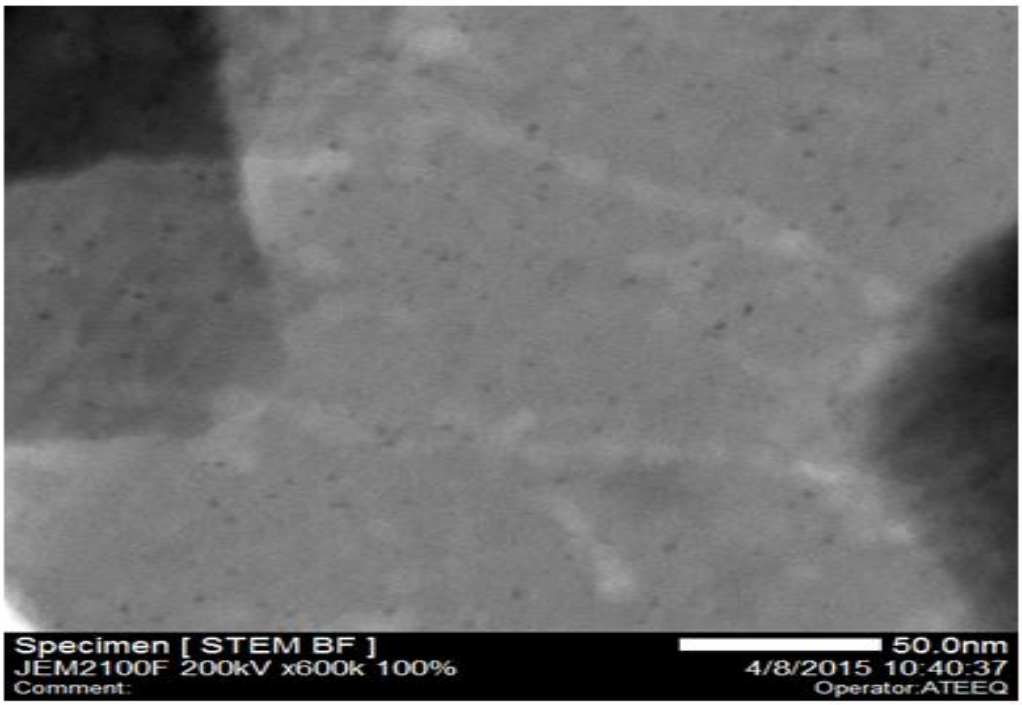


**Figure 4.3 Scanning Transmission Electron Micrograph for 0.32 wt. % RuPdECY-3B**

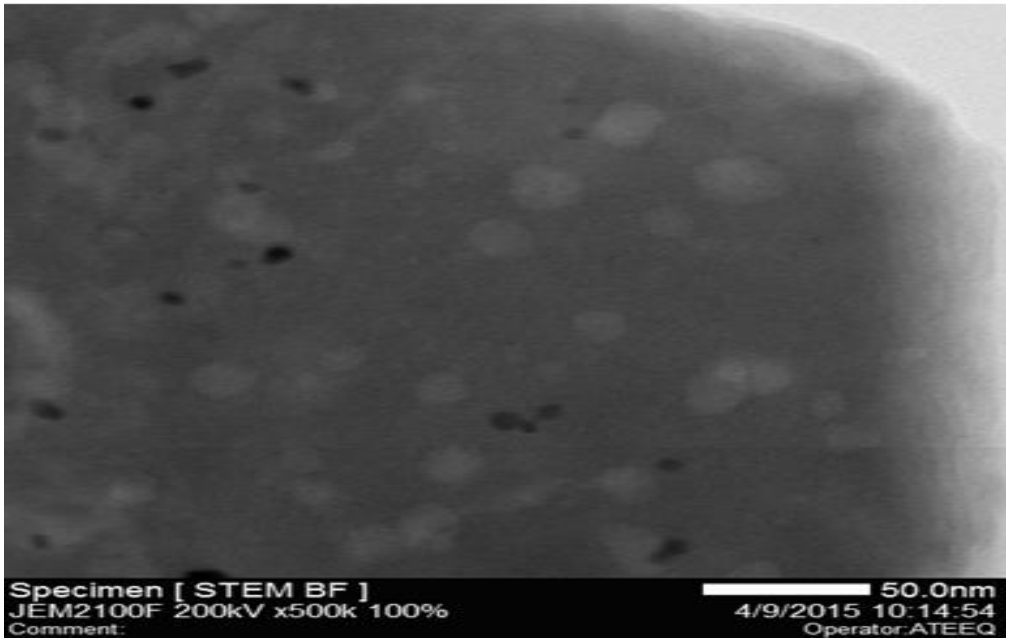


**Figure 4.4 Scanning Transmission Electron Micrograph for 0.16wt% RuPdECY-4B**

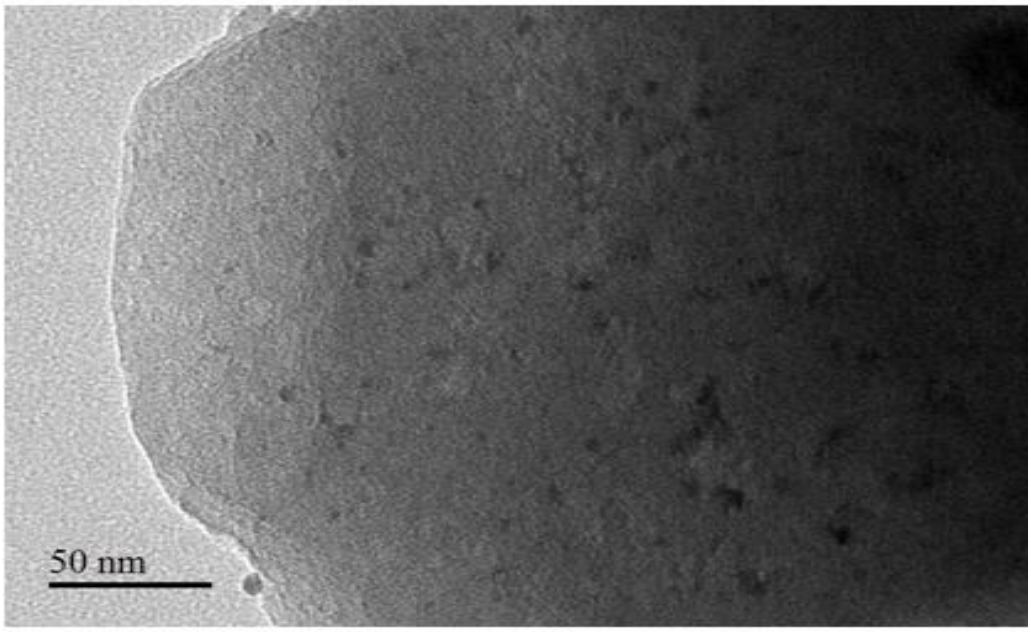


**Figure 4.5 Transmission Electron Micrographs 1.08 wt% RuPd-Al2O3-YD1**

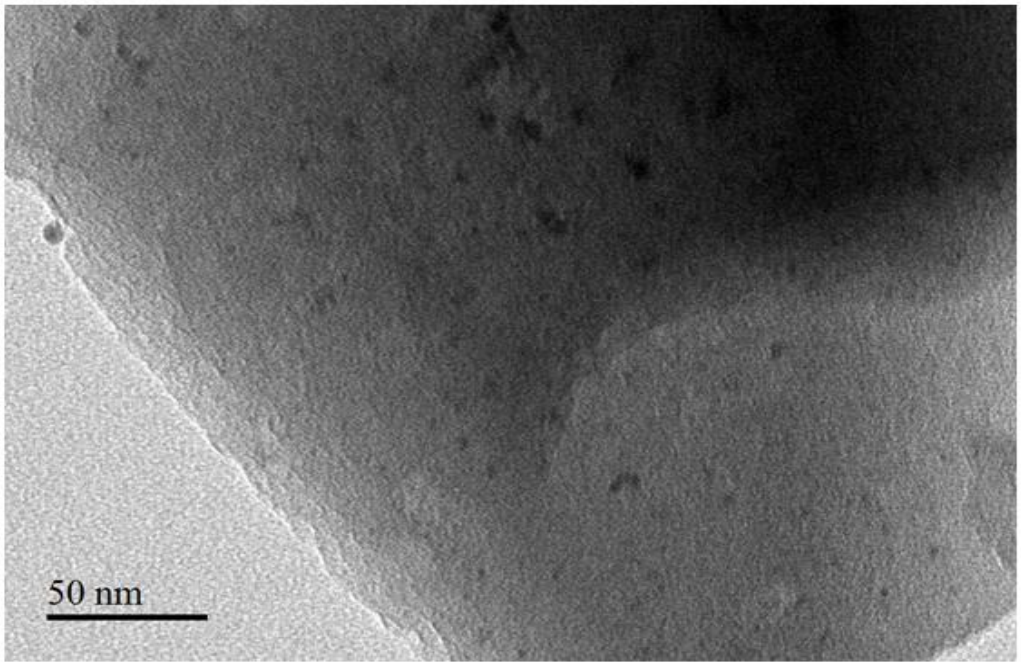


**Figure 4.6 Transmission Electron Micrographs 0.72 wt% RuPd-$Al_2O_3$-YD2**

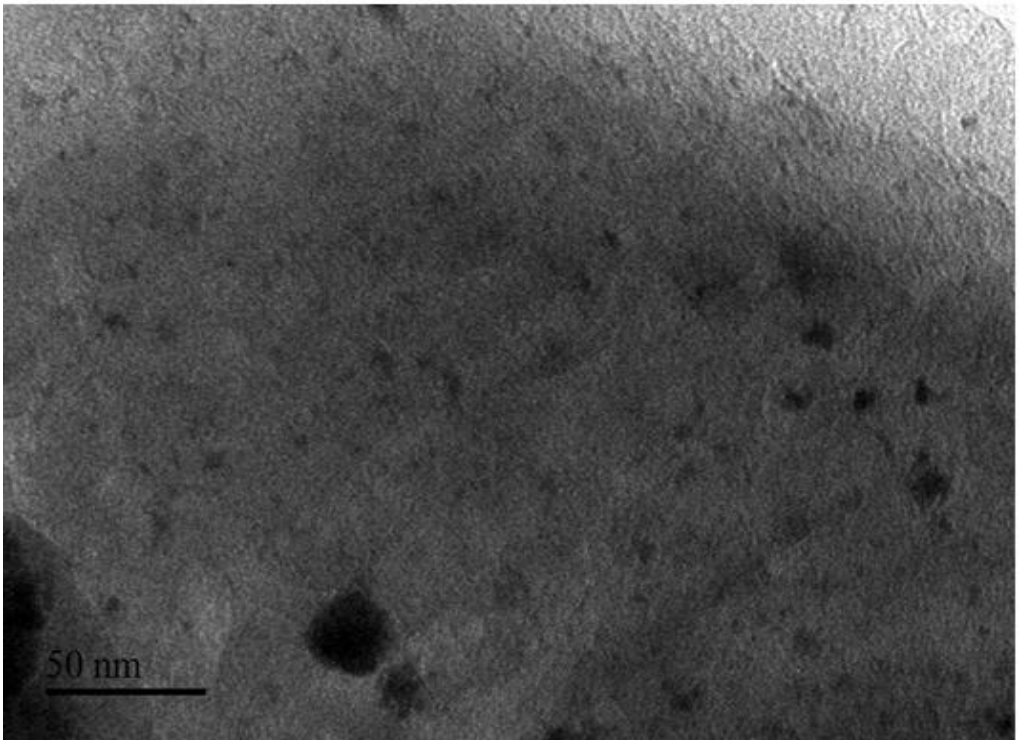


**Figure 4.7 Transmission Electron Micrographs 0.50 wt% RuPd-$Al_2O_3$-YD3**

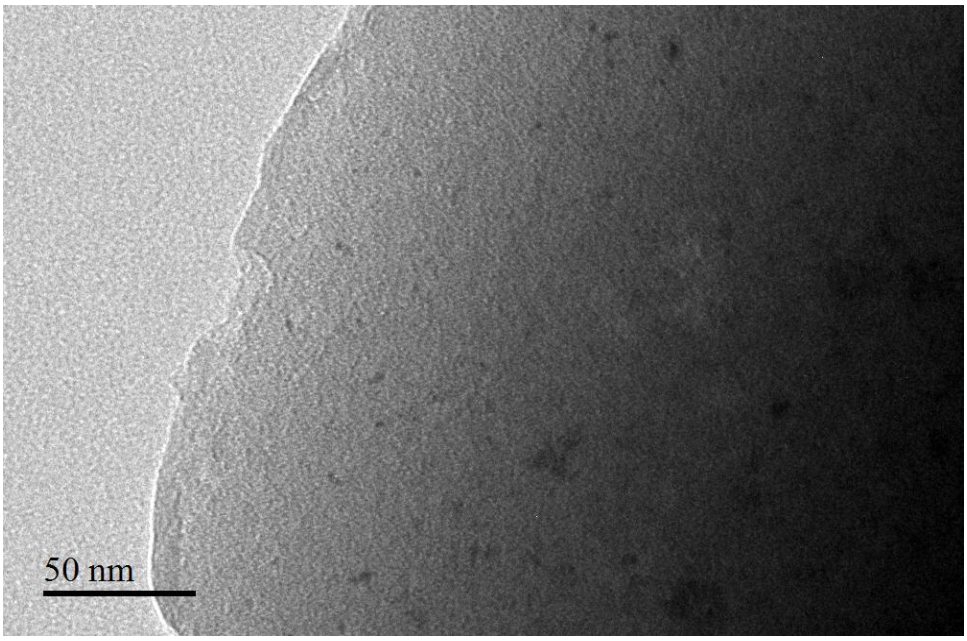


**Figure 4.8 Transmission Electron Micrographs 0.20 wt% RuPd-$Al_2O_3$-YD4**

## 4.5 X-Ray Diffraction profiles

The X-ray diffraction profiles of Y zeolite, before and after ion exchange treatment were characterized by powder X-ray diffraction. The XRD profiles obtained for the different catalysts are depicted in figure 4.18-19. The profiles obtained for Y zeolite support are in agreement with the characteristic diffraction patterns of this zeolite, in terms of relative intensities of the peaks and their positions. A well crystallized framework and low background observed can be attributed to the absence of amorphous phase in the support.

For all the catalysts prepared, there was no peak correlating to the metals. This observation suggests that there was no agglomeration of metals that can lead to detectable peaks; therefore, an excellent dispersion of metals is a reasonable conclusion from this observation [20, 39, and 40].

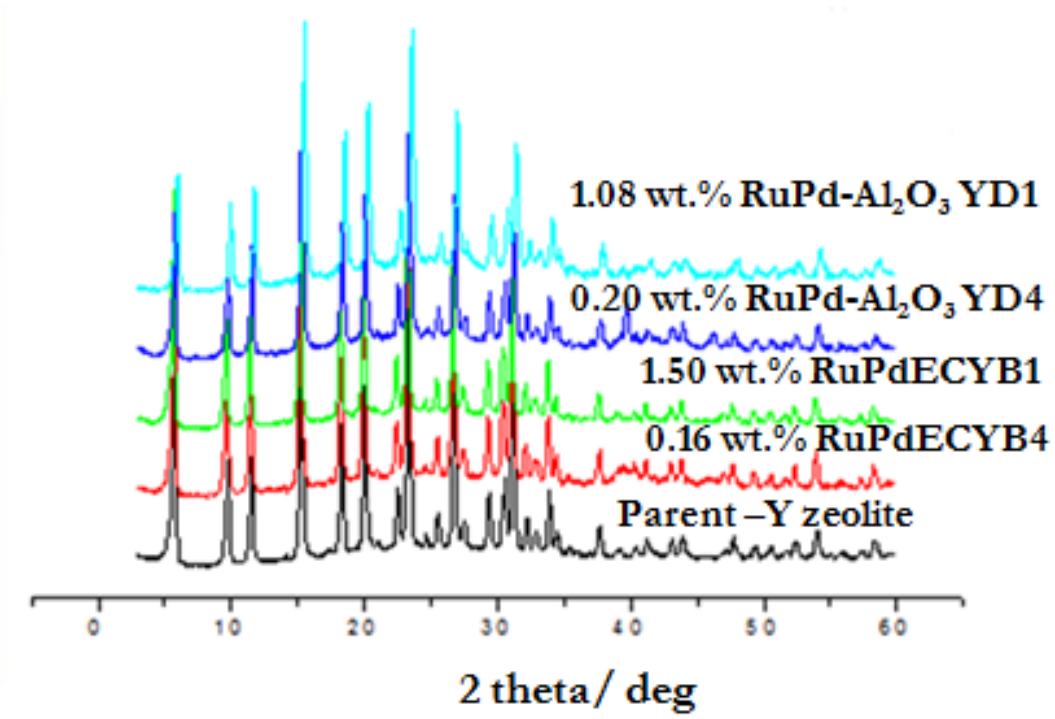


**Figure 4.9 Powder XRD profiles of the prepared bimetallic catalysts**

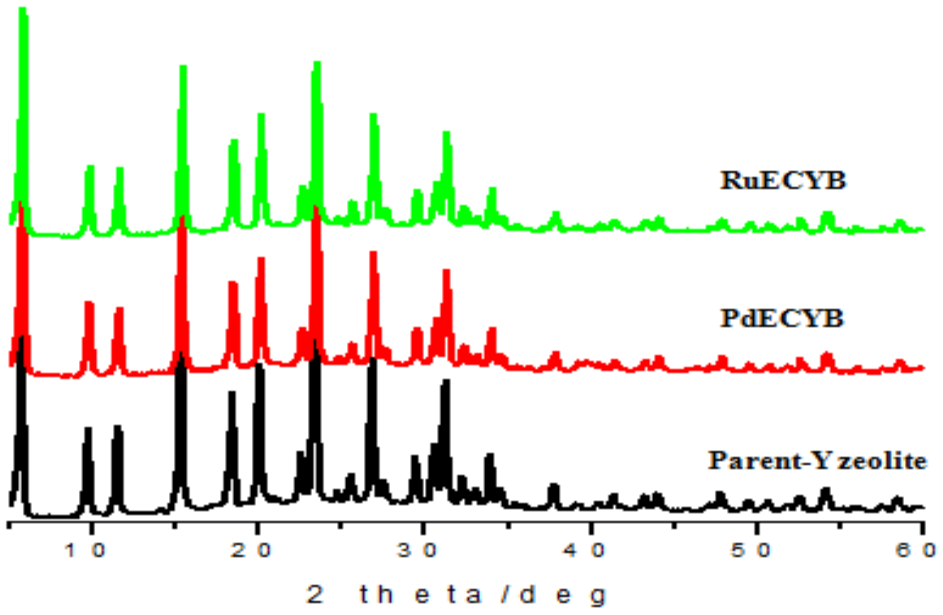


**Figure 4.10 Powder XRD profiles of prepared single-metal catalysts.**

## 4.6 Product Analysis

Prior to feeding the samples into the GC, the system was calibrated using known concentrations of expected products. Further confirmation of retention times was established using gas chromatography mass spectrometry (GC-MS) fitted with column of the same specifications as GC-FID as detailed in section 3.4.3. The figure 4.20 show the chromatogram of a representative liquid sample collected during reaction. The different representative products, their retention times and their fragmentation patterns are as depicted in figure 4.20-25. These figures are fragmentation patterns of the feed (naphthalene) and major products such as tetralin, decalin, benzene (monoaromatics) and cyclohexane and upon which this research is set to investigate.

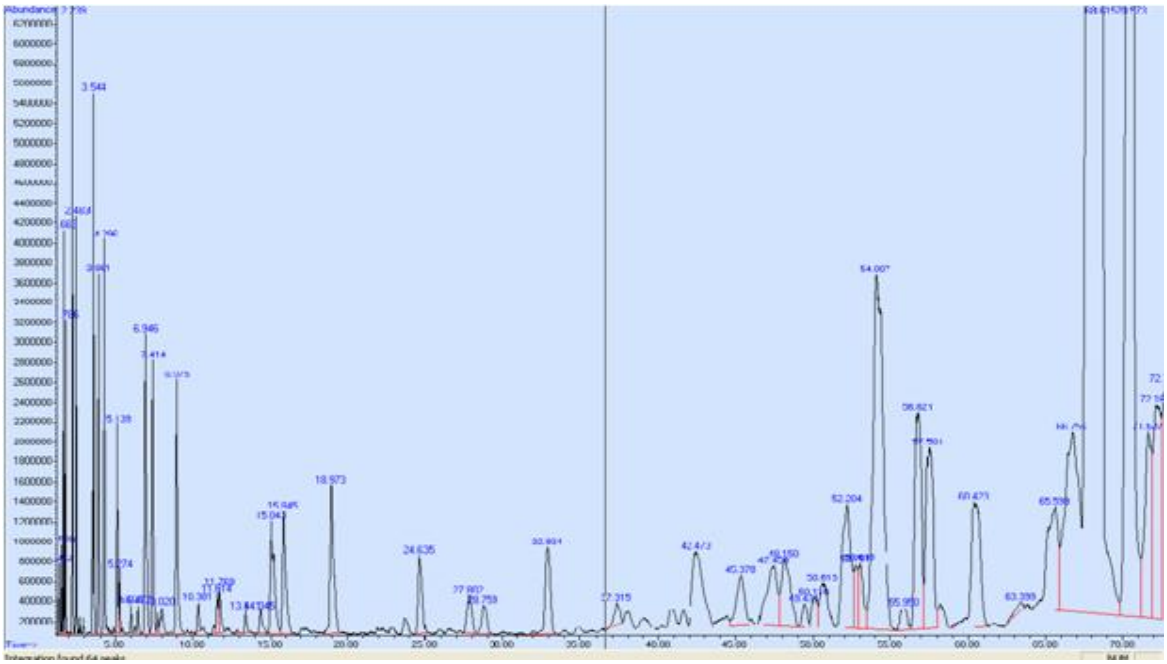

**Figure 4.11 GC-MS chromatogram of hydrocracking products**

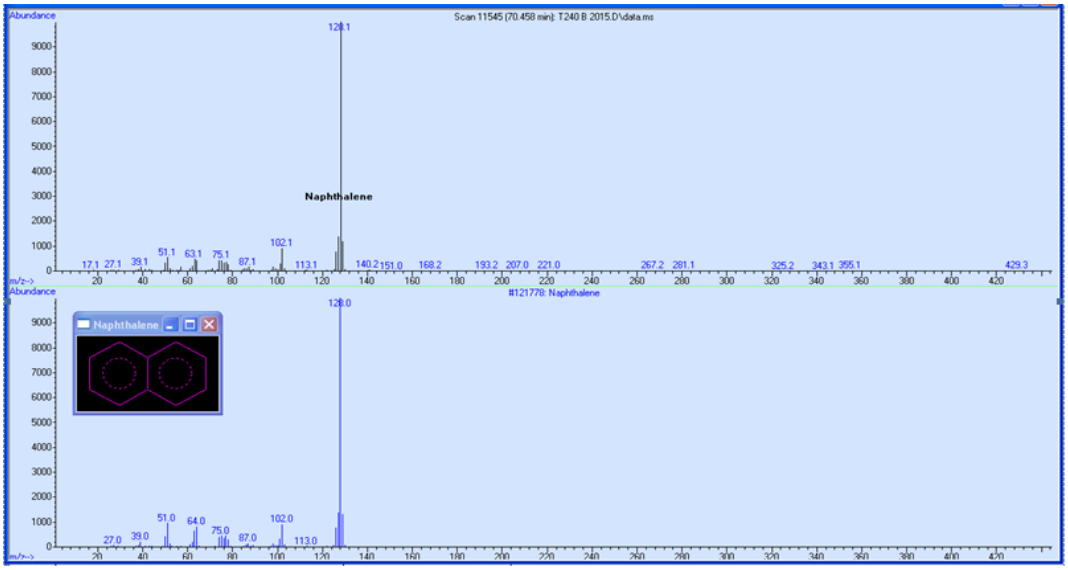


**Figure 4.21 Gas Chromatographic Mass Spectrometry fragmentation pattern of naphthalene**

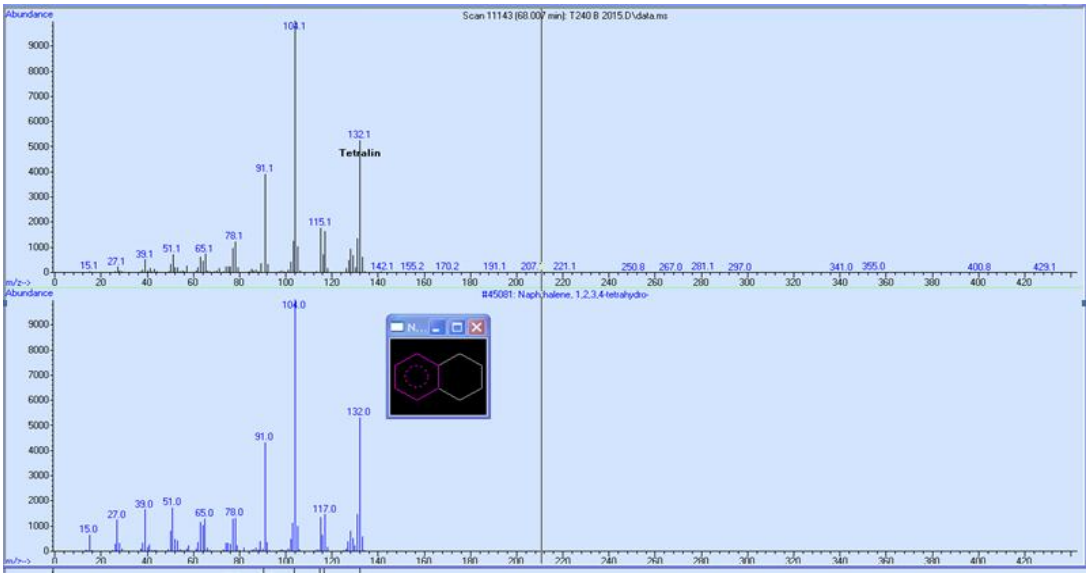


**Figure 4.22 Gas Chromatographic Mass Spectrometry fragmentation pattern of tetralin**

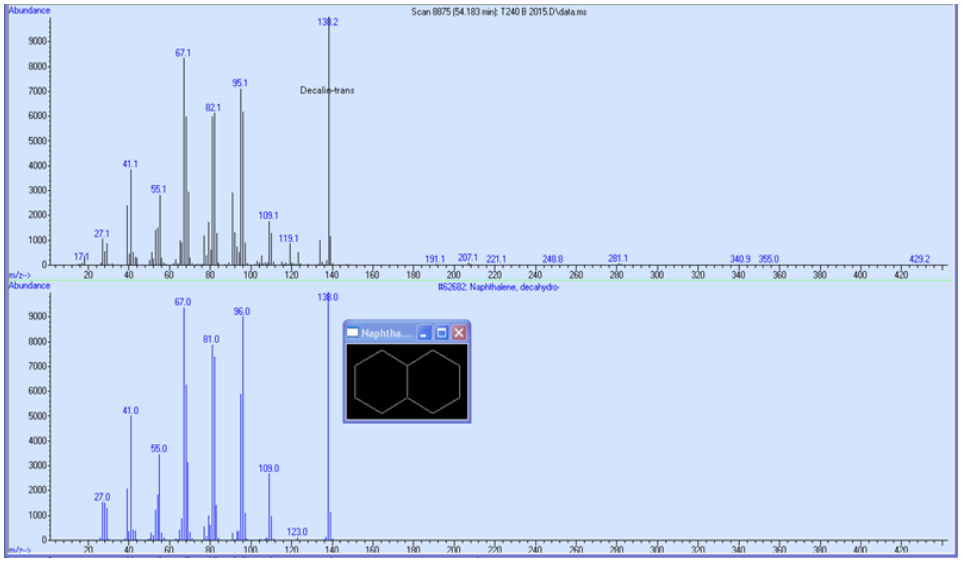


**Figure 4.12 Gas Chromatographic Mass Spectrometry fragmentation pattern of Decalin(trans)**

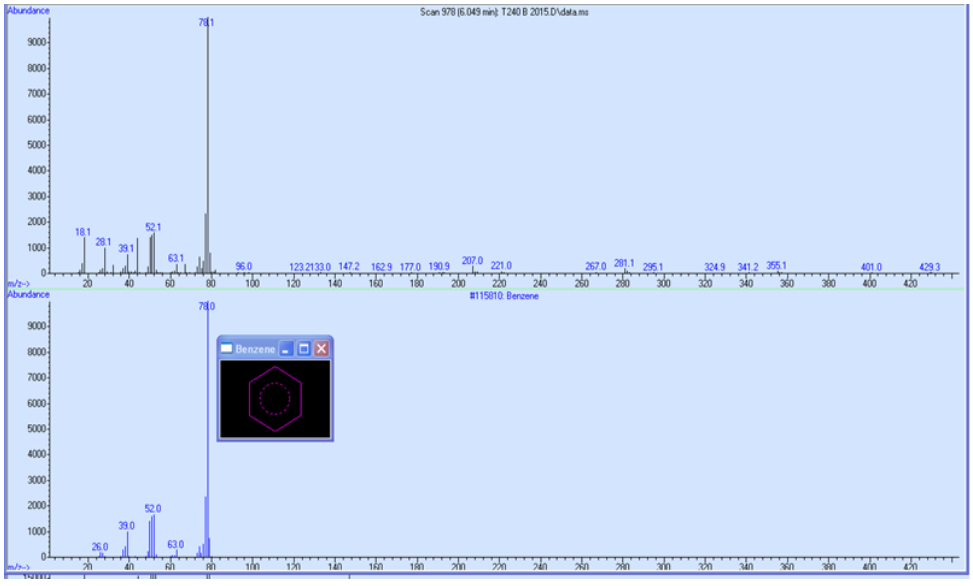


**Figure 4.13 Gas Chromatographic Mass Spectrometry fragmentation pattern of benzene**

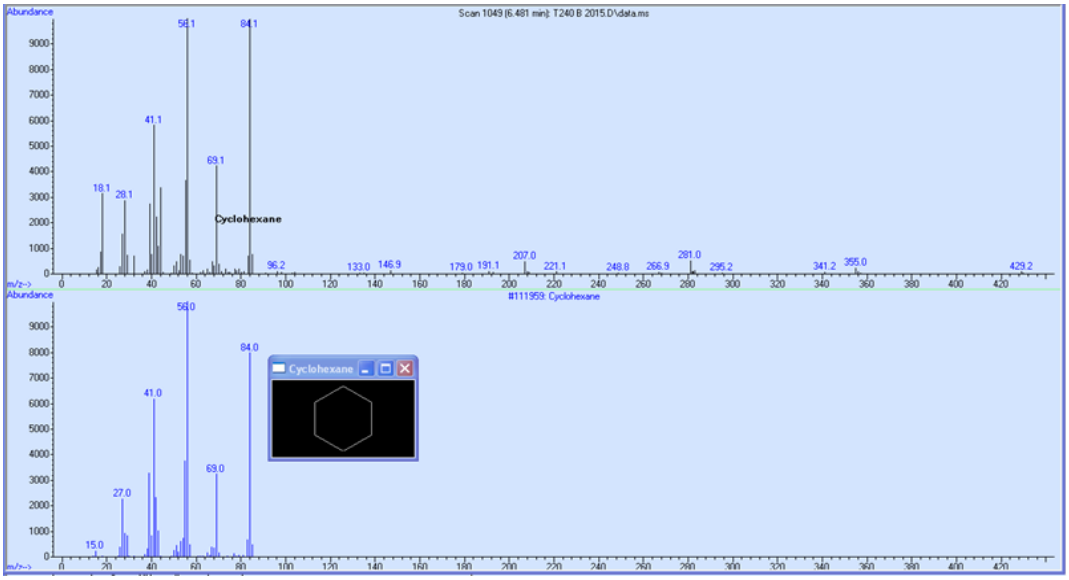


**Figure 4.14 Gas Chromatographic Mass Spectrometry fragmentation pattern of cyclohexane**

## 4.7 Product classification

Due to several elementary reaction steps, several products were identified including intermediates and isomers. These products resulted from either partial or complete hydrogenation and cracking of naphthalene. Although, there were light hydrocarbon products like straight-chain butane, pentane, and hexane. They were believed to be from the cracking of the dodecane used in preparing the feed. In addition, the cracking of dodecane was hindered by the presence of naphthalene because it is more nucleophilic than dodecane on both the metal and Bronsted acid active sites. Therefore, the light hydrocarbons formed are not considered in product distribution (table 4.5) and calculations [41]. The different classes of products identified and the compounds constituting them are as shown in table 4.5

**Table 4.5 Classes of identified products and their constituent hydrocarbons**

| **CLASS** | **COMPOUNDS*** |
|---|---|
| Tetralin | Tetralin,1-methylindane, 2-methylindane |
| Decalins | Decalin (cis and trans) |
| Monoaromatics | Benzene, toluene, ethylbenzene, xylenes (ortho, meta and para) |
| Cyclohexanes | Cyclohexane, methylcyclopentane, 1,2-dimethylcyclohexane,<br>1-methylcyclohexene, ethyl, propyl, butyl-cyclohexene. |

*major compounds identified by GC which account for ≥ 95 of the feed at the start of reaction.

## 4.8 Hydrocracking activity of the prepared catalysts

The figure 4.26 shows the conversion of naphthalene via hydrocracking process using the reaction conditions detailed in table 3.. As the percentage conversion of naphthalene increases, a direct translation is seen in the increasing amount of products formed with Tetralin being the highest followed by Decalins then Monoaromatics and Cyclohexanes the least. This clearly indicates that hydrogenation process is faster than hydrocracking. Furthermore, hydrogenation is an exothermic process that requires lower activation energy barrier than cracking process where cleavage of sigma bond is involved [39-43]. The hydrogenation and hydrocracking activities increase throughout the reaction period and with optimum yet to be reached after four hours reaction period. This indicates that higher conversion of the feed is still possible before deactivation. This also confirmed maintenance of the crystalline structure of the catalyst as discussed in section 4.13 and shown in the XRD pattern of the spent catalyst in figure 4.31

A maximum conversion of 88.3 % of naphthalene was achieved on ruthenium single metal-based catalyst and 86.4 % for Ru-Pd bimetallic-based catalyst. With Pd single metal catalyst, the conversion achieved is less than 20 % which is slightly higher than what is observed for bare supports employed in this study. Nonetheless, the thio-tolerant activity was better with bimetallic catalyst than single metal Ru catalyst as discussed in section 4.12. This confirms the promotional effect of bimetallic catalyst system [20].

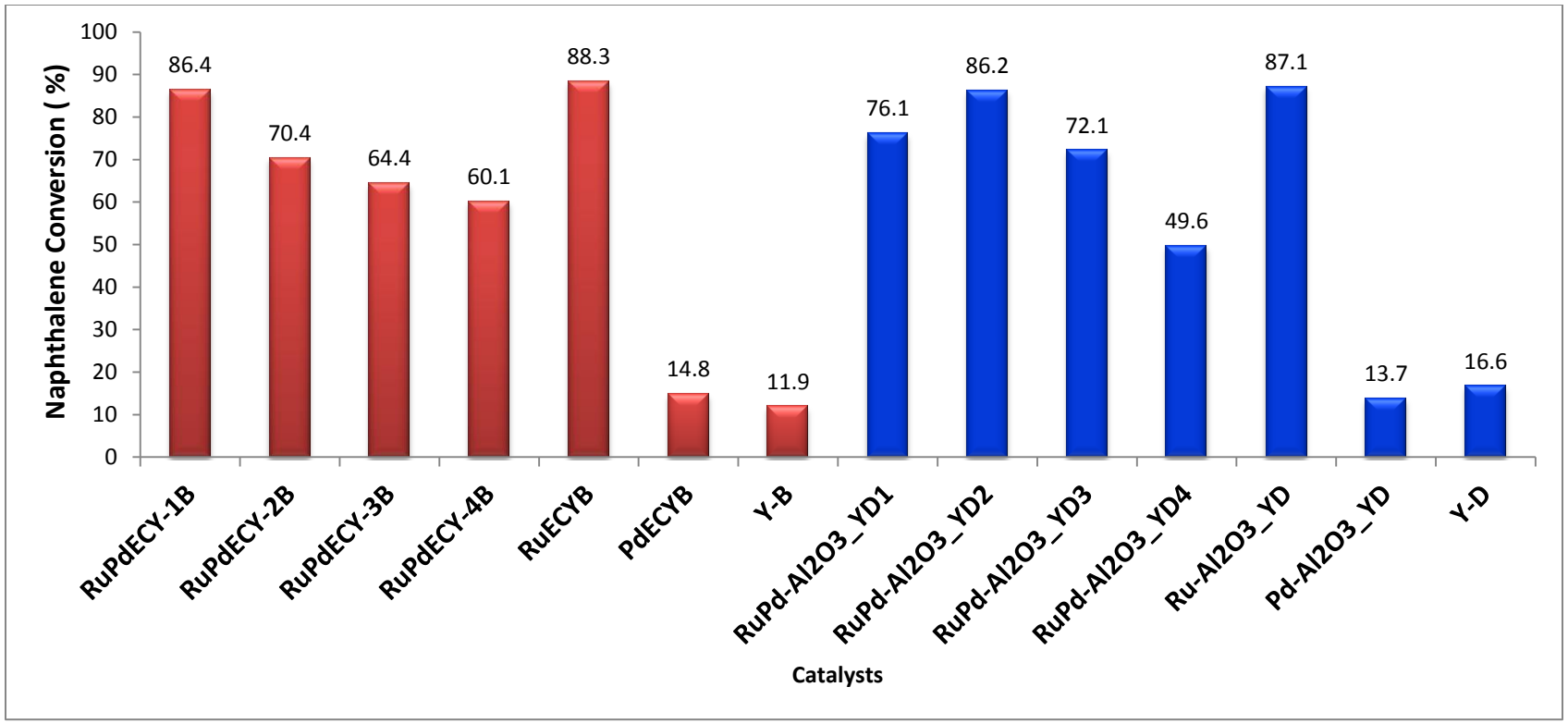


**See table 3.1 for reaction conditions**

**Figure 4.15 Percentage conversion of naphthalene of various prepared catalysts after 4 hrs.**

## 4.9 Catalyst selectivity

The selectivity of all the prepared catalysts, irrespective of the nature of support and metal loading, follows the same trend in product distribution such that hydrogenation products like Tetralin and Decalins are yielded in larger amount than cracking products; Monoaromatics and Cyclohexanes. Tetralin yield is the highest followed by Decalins, Monoaromatics and the least being Cyclohexanes. This observation is shown in figure 4.29 and table 4.6 which was further confirmed by the rate constants obtained for the formation of each category of products as discussed in section 4.14 which elucidate the reaction kinetics.

**Table 4.6 Selectivity of the prepared catalyst to naphthalene hydrocracking products**

| Catalyst | Tetralin (%) | Decalins (%) | Monoaromatics (%) | Cyclohexanes (%) | Naphthalene conversion (%) |
|---|---|---|---|---|---|
| RuPdECY-1B | 45.5 | 27.8 | 26.0 | 0.7 | 86.4 |
| RuPdECY-2B | 53.9 | 25.4 | 19.9 | 0.8 | 70.4 |
| RuPdECY-3B | 47.9 | 25.5 | 26.0 | 0.6 | 64.4 |
| RuPdECY-4B | 46.0 | 24.4 | 29.1 | 0.5 | 60.1 |
| RuECY-B | 37.9 | 30.6 | 30.8 | 0.7 | 88.3 |
| PdECY-B | 46.9 | 31.0 | 22.2 | 0.9 | 14.8 |
| RuPd-$Al_2O_3$_YD1 | 46.5 | 28.3 | 24.7 | 0.5 | 76.1 |
| RuPd-$Al_2O_3$_YD2 | 45.3 | 32.4 | 21.3 | 1.0 | 86.2 |
| RuPd-$Al_2O_3$_YD3 | 56.1 | 27.5 | 15.8 | 0.6 | 72.1 |
| RuPd-$Al_2O_3$_YD4 | 60.4 | 24.6 | 14.4 | 0.6 | 49.6 |
| Ru-$Al_2O_3$_YD | 37.0 | 31.6 | 30.4 | 1.0 | 87.1 |
| Pd-$Al_2O_3$_YD | 32.0 | 45.9 | 21.1 | 1.0 | 13.7 |

## 4.10 Effect of metal loading on conversion of naphthalene

In any bifunctional catalyst for hydrocracking process, metal active sites play a crucial role in the hydrogenation of unsaturated hydrocarbons. This indeed is the first step in hydrocracking process of cyclic aromatic compounds before subsequent ring opening [17-20].

The amount of metal loaded therefore is expected to have significant effect among other factors on the level of conversion that can be achieved. We investigated the influence of metal loading by preparing catalyst with different amount of metal nanoparticles of ruthenium and palladium with more palladium than ruthenium in all cases. For all the prepared catalysts, the metal loadings are as stated in table 4.1-3

From figures 4.27 and 4.28, the amount of naphthalene in the feed decreases with metal loading which indicates more conversion of naphthalene with catalyst having more metal loading. RuPdECY-1B with 1.15 wt% have reached minimum amount of naphthalene as expected in the B-series. For the D-series, a slight change in the trend was observed as RuPd-$Al_2O_3$_YD2 with 0.72 wt% instead RuPd-$Al_2O_3$_YD1 (1.08 wt %) of reached minimum amount of naphthalene over the reaction period of 4 h (figure 4.26). This could be attributed to the 0.72 wt % is the optimum metal loading and that extra loading only goes into the pores of the supports and block it thus reducing its activity [15].

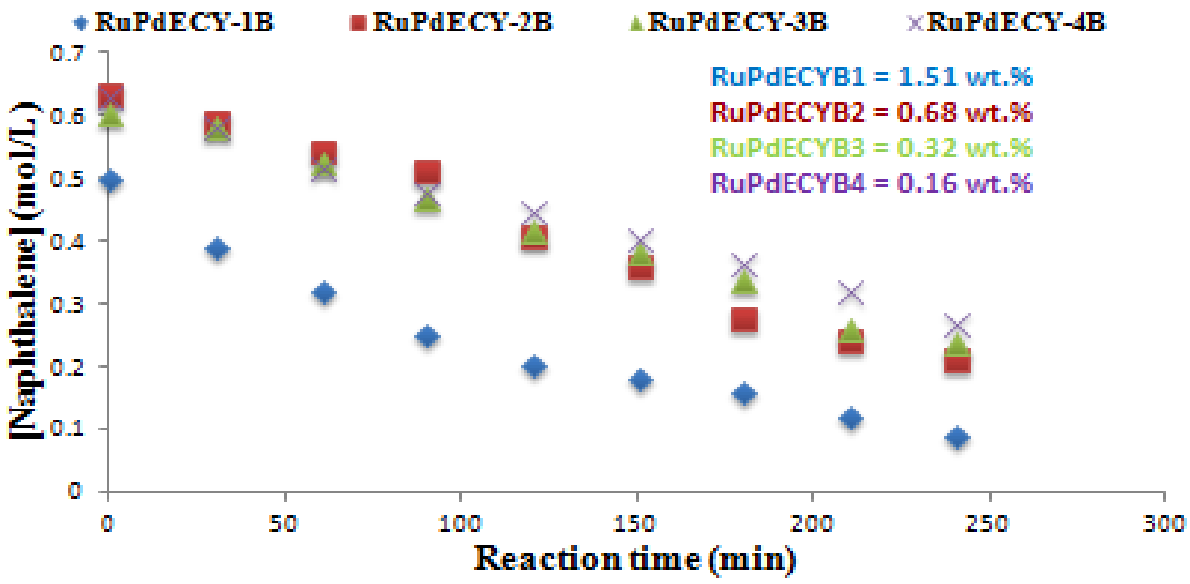


**Figure 4.16Amount of naphthalene over the period of reaction for bimetallic-based RuPdECYB catalysts**

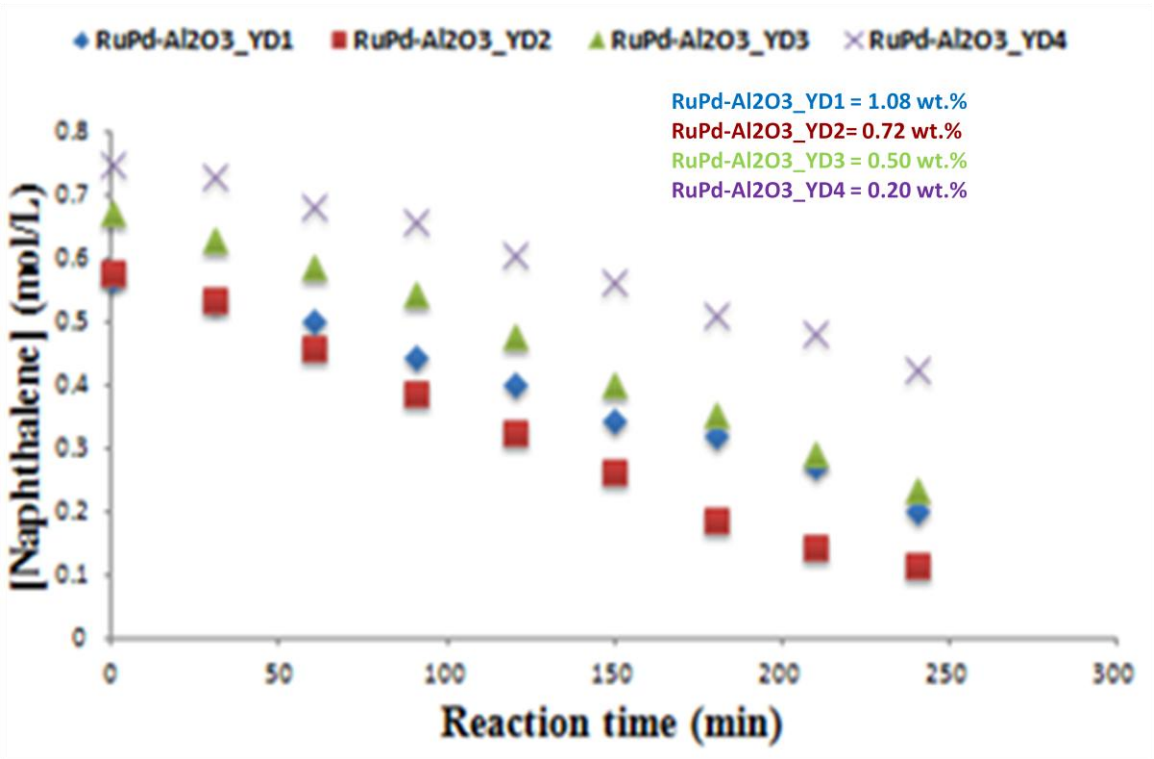


**Figure 4.17 Amount of naphthalene over the period of reaction for bimetallic-based RuPd-$Al_2O_3$_YD catalysts**

## 4.11 Effect of support acidity on conversion of naphthalene

Another very vital functionality in a bifunctional catalyst is the acid sites (Bronsted and lewis). The acid sites especially the Bronsted is responsible for cracking activity in the hydrocracking reaction. However, a need to selectively control the ring opening process and at the same time minimize the amount of gases produced during the refining process, an optimum acidity therefore is a very key factor to be put into consideration [17]. The B-series of the prepared catalysts are RuPdECY-1B, RuPdECY-2B, RuPdECY-3B and RuPdECY-4B with naked calcined Y-zeolite support which is more acidic than the D-series RuPd-$Al_2O_3$_YDI, RuPd-$Al_2O_3$_YD2, RuPd-$Al_2O_3$_YD3 and RuPd-$Al_2O_3$_YD4 with alumina-coated calcined Y-zeolite as support. The controlled acidity by alumina is confirmed by the higher amount of $H_2$ uptake and better metal dispersion because the metal-support interaction is lower compared to the catalysts with bare zeolite support (B-series) as shown in table 4.4

As shown in figure 4.29, the yield of hydrogenation products (Tetralin and Decalins) is generally more for the less acidic alumina-coated D-series catalysts than what is achieved with more acidic B-series. Also, the B-series yielded more cracking products (Monoaromatics and Cyclohexanes). This is expected since the acid site is implicated in cracking activity [19, 20].

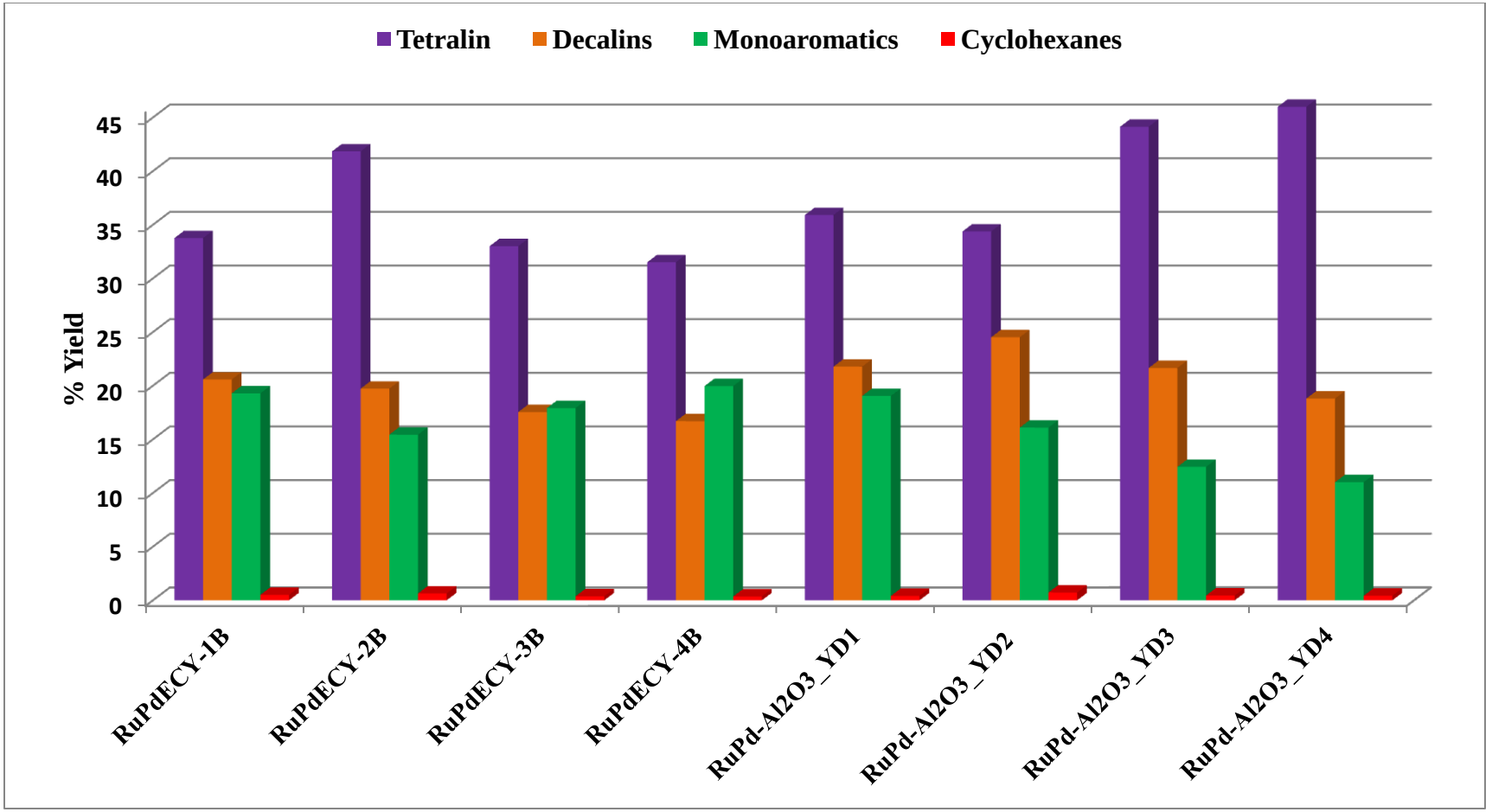


**Figure 4.18 Percentage yield of hydrocracking products for naked and alumina-coated bimetallic-based catalysts**

## 4.12 Thio-tolerant Activity

Compounds of sulfur in crude oil are the most abundant heteroatomic organo-compounds which their removal is very challenging and pose a great danger to the environment. Sulfur compounds are known to poison catalysts employed in petroleum refining process. These organosulfur compounds are present as thiols, thiophene and its derivatives and sulfides.

The thio-tolerant activity of RuPdECY-1B and RuECYB being two of the most active catalysts were evaluated with a feed containing 1000 ppm of DBT using optimal experimental conditions; 300 °C, 5 MPa initial pressure of hydrogen gas and for 4 hours. As depicted in figure 4.30, with 1000 ppm of DBT these catalysts showed no significant deactivation, with very insignificant change in conversion without changing pattern of yields of different products. This observation could result from the sulfur produced in the HDS reaction of DBT that is not directly released as $H_2S$ but rather could be present in the catalyst structure [20, 47]. So, palladium or ruthenium metals are modified by the presence of sulfur, possibly forming palladium or ruthenium sulfide with hydrogenation properties. However, the decrease in conversion for bimetallic RuPdECY-1B (5.0 %) is less compared to single metal RuECY (10.4 %). This indicates that the bimetallic-based catalyst system is a better thio-tolerant and more ideal catalyst for hydro-conversion of poly-aromatics than single metal counterpart [17].

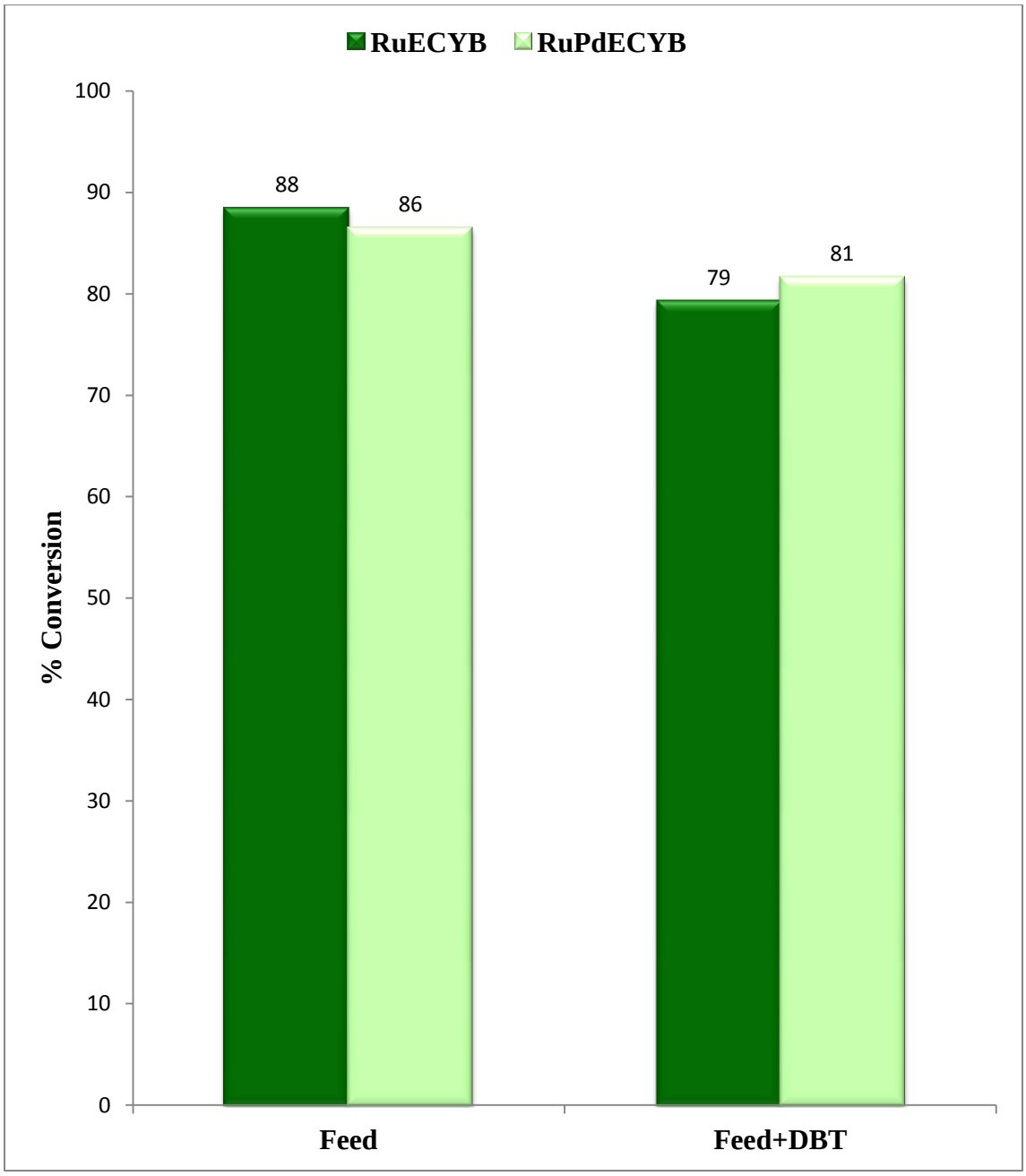


**Figure 4.30 Percentage conversion of naphthalene in the presence and absence of dibenzothiophene for RuECYB and RuPdECY-1B**

## 4.13 Catalysts stability and recyclability

The stability of the catalyst is tested by checking the powder X-Ray diffractogram of the catalysts after 4 hours of hydrocracking reaction under the set reaction condition. The diffractogram of spent catalysts when compared those of the freshly prepared and parent Y-zeolite, there is no significant difference observed in their intensities as depicted in figure 4.31. This observation is an indication that the catalysts can still go through more hydrocracking cycles without significant decrease in their activities.

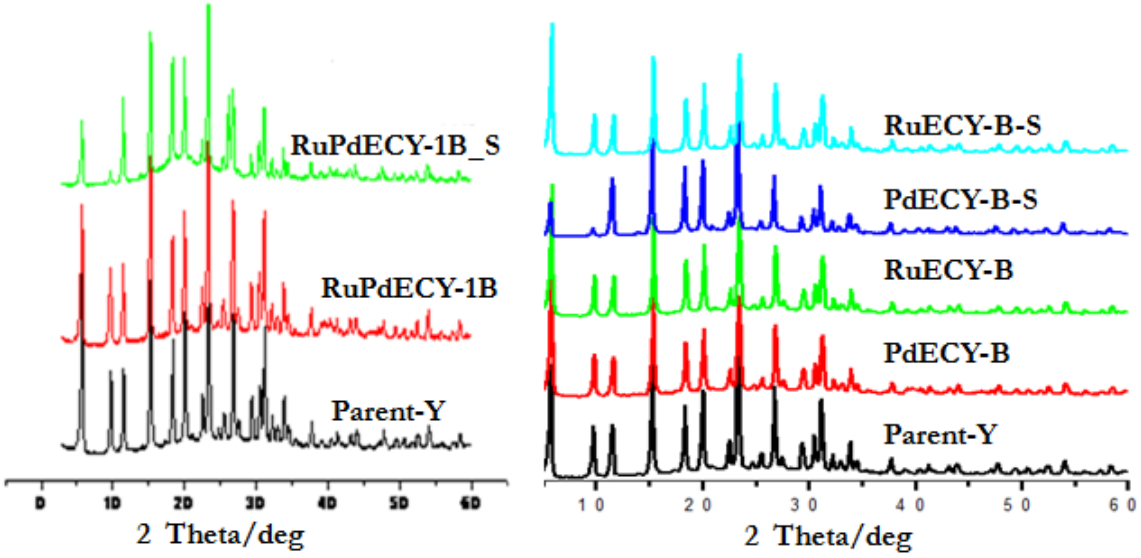


**Figure 4.19 Powder X-Ray diffractogram of some prepared catalysts before and after reaction (S = spent)**

## 4.14 Kinetic model

In order to further study the hydrocracking process qualitatively, a reaction scheme is designed based on major products identified which are grouped as; tetralin, decalins, monoaromatics and cyclohexanes as depicted in figure 4.32.

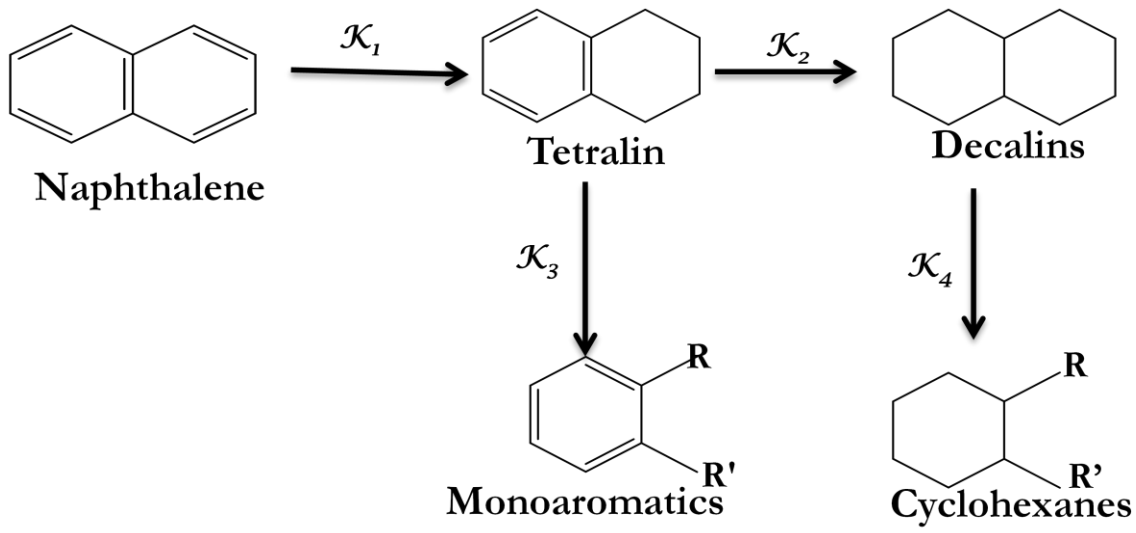


**Figure 4.20 Hydrocracking reaction scheme**

The various hydrogenation and hydrocracking products are classified into four groups as shown in figure 4.32. For a well detailed kinetic model for naphthalene hydrocracking, several reaction steps which are elementary in nature are involved; this gives rise to a very complex kinetics which is extremely difficult to follow. In order to simplify this, the reaction steps and products are assigned into groups which are referred to as lumps and are independent entity. This is referred to as lumped kinetics approach as shown above [46].

To obtain rate constants for all the various steps involved in the reaction scheme proposed in figure 4.32 and to further reveal some vital informations about the reactions, a mathematica software (<Statistics`NonlinearFit`) at 95% confidence region was used to solve all the rate expressions as written below:

- Rate of disappearance of naphthalene; $-d\frac{[Nph]}{dt} = k1[Nph]$
- Rate of formation of Tetralin; $d\frac{[tet]}{dt} = k1[Nph] - (k2 + k3)[tet]$
- Rate of formation of Decalins; $d\frac{[Dec]}{dt} = k2[tet]$- $k4[Dec]$
- Rate of formation of Monoaromatics; $d\frac{[monoaro]}{dt} = k3[tet]$
- Rate of formation of cyclohexanes; $d\frac{[Cyclo]}{dt} = k4[Dec]$

Naphthalene (Nph); tetralin (tet); decalins (Dec); monoaromatics (monoaro); Cyclohexanes (Cyclo).

**Table 4.7 Rate constants of hydrogenation and cracking reactions**

| Catalyst | Hydrogenation rate constants | | Cracking rate constants | |
|---|---|---|---|---|
| | $K_1 x10^3 (min^{-1})$ | $K_2 x10^3 (min^{-1})$ | $K_3 x10^3 (min^{-1})$ | $K_4 x10^3 (min^{-1})$ |
| RuPdECY-1B | 6.54 | 5.01 | 1.97 | 0.15 |
| RuPdECY-2B | 3.80 | 2.48 | 1.73 | 0.18 |
| RuPdECY-3B | 3.22 | 3.52 | 2.69 | 0.12 |
| RuPdECY-4B | 2.75 | 2.25 | 2.18 | 0.13 |
| RuPd-$Al_2O_3$YD1 | 3.13 | 2.02 | 1.33 | 0.40 |
| RuPd-$Al_2O_3$YD2 | 5.45 | 2.68 | 1.20 | 0.70 |
| RuPd-$Al_2O_3$YD3 | 3.48 | 2.07 | 0.87 | 0.10 |
| RuPd-$Al_2O_3$YD4 | 2.03 | 2.05 | 1.15 | 0.61 |

From table 4.7, rate constants $K_1$ and $K_2$ correspond to hydrogenation reactions which convert naphthalene to Tetralin and Decalins respectively. The rate of conversion to Tetralin is the fastest as shown by its K-values ($K_{1)}$ and the values decreases down the B-series catalysts which can conveniently be attributed to the amount of metal loading as it decreases from RuPdECY-1B to RuPdECY-4B. The hydrogenation process occurs majorly on the metal active sites [20]. However, the same trend was not seen in the case of D-series catalyst which may be due to its very weak metal-support interaction caused by alumina coating.

Regardless of the amount of metal loading or the nature of the supports, the rate constants observed for hydrogenation reactions ($K_1$ and $K_2$) are higher compare to cracking ($K_3$ and $K_4$) (Table 4.7). This is further buttressed by the higher yield and selectivity of all the catalysts to hydrogenation products (Tetralin and Decalins) as seen in table 4.6 and figure 4.29. Other reasons for these observations are the fact that hydrogenation is an exothermic process in which less energy is required compared to cracking process which is endothermic and therefore, higher amount of energy would be required to cleave a bond in order to open a ring [16-20].

### 4.14.1 Agreement between experimental and calculated reaction data

With the aid of mathematica software, a good agreement between experimental (red dots) and calculated values ( blue line was observed) wih their unique K-values.

The hydrocracking process shows best fit for Langmuir-Hinshelwood mechanism considering the fact that the amount of the naphthalene in the feed is small and the reaction was perfomed under the passage of excess hydrogen thus gives a first-order kinetics. In figure 4.33-36, for the B-series catalysts,the plots of concentration of tetralin against reaction time showed that the rate passed through the maximum in each of the plots and then stated falling. This is observed clearly for tetralin within the 4 hours of reaction because its formation is faster than other products. Similarly, this same observation was observed for the D-series catalysts which are also shown in figures 4.37-40.

However, some fall-off points were noted as seen in the plots which could be due to several factors from reaction exothermicity, tailing peaks from GC analysis, and many products interactions. This observation further confirms the complexity of hydrocracking reaction kinetics.

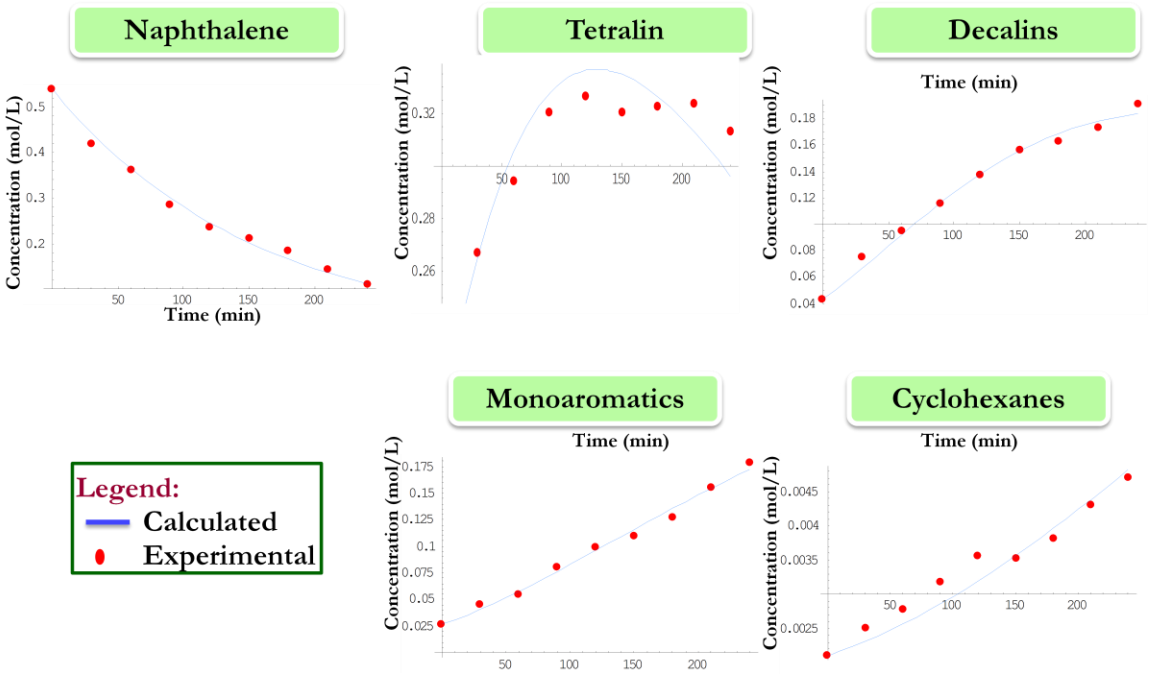


**Figure 4.21 Experimental versus calculated data for RuPdECY-1B**

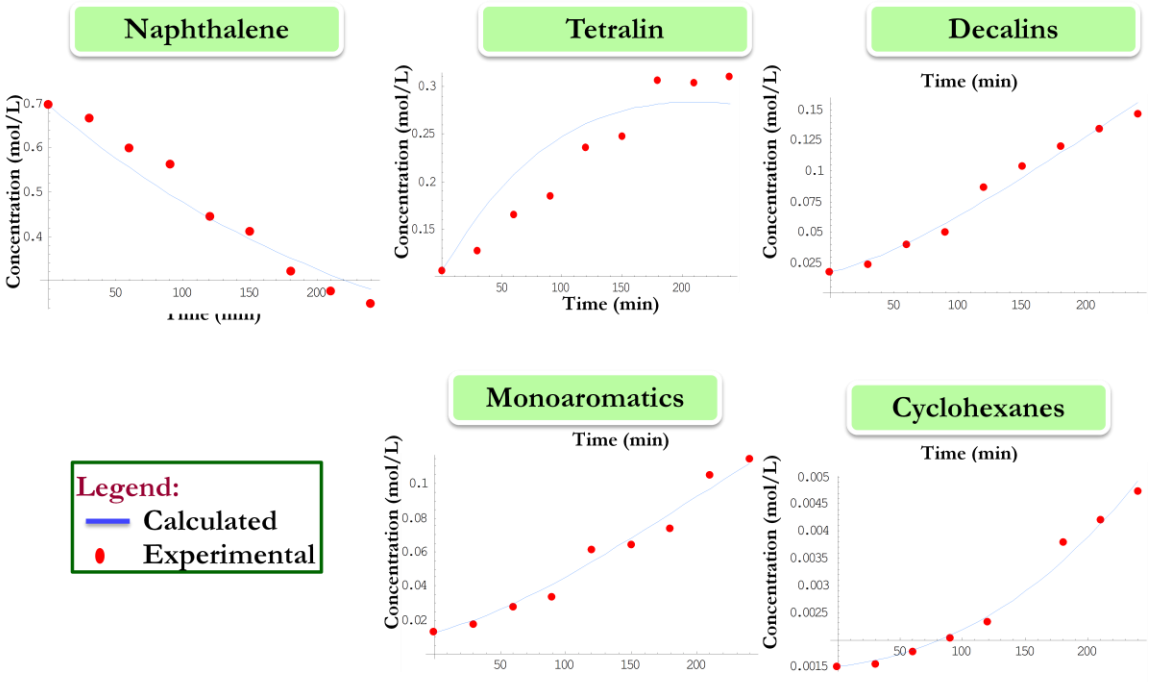


**Figure 4.22 Experimental versus calculated data for RuPdECY-2B**

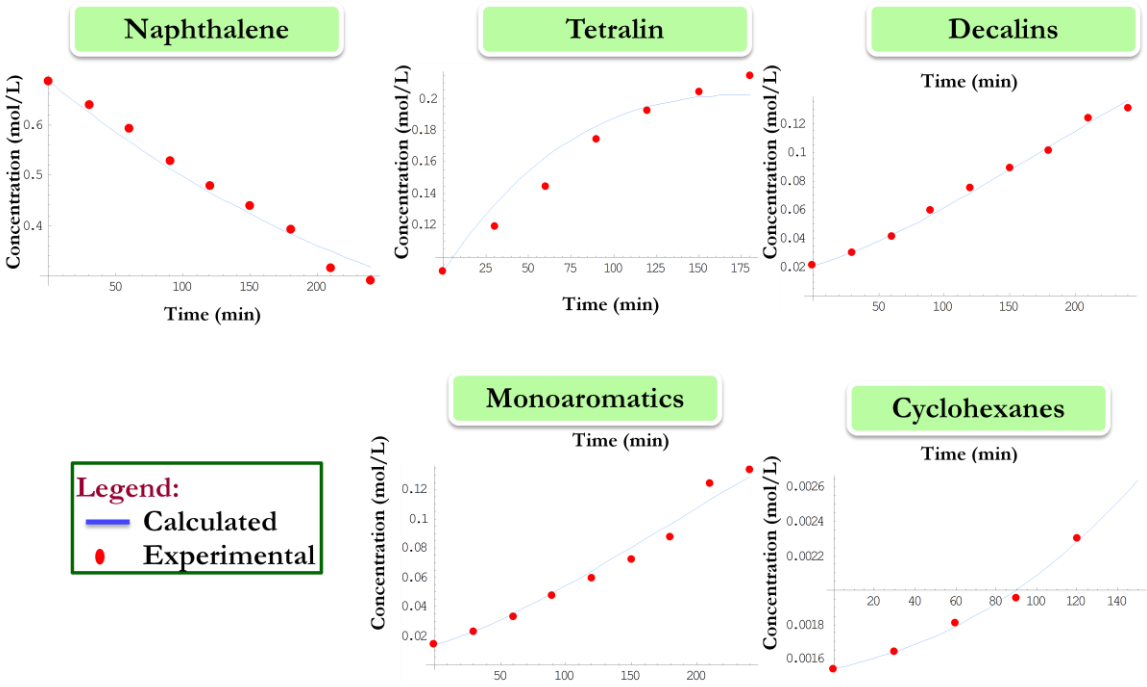


**Figure 4.23 Experimental versus calculated data for RuPdECY-3B**

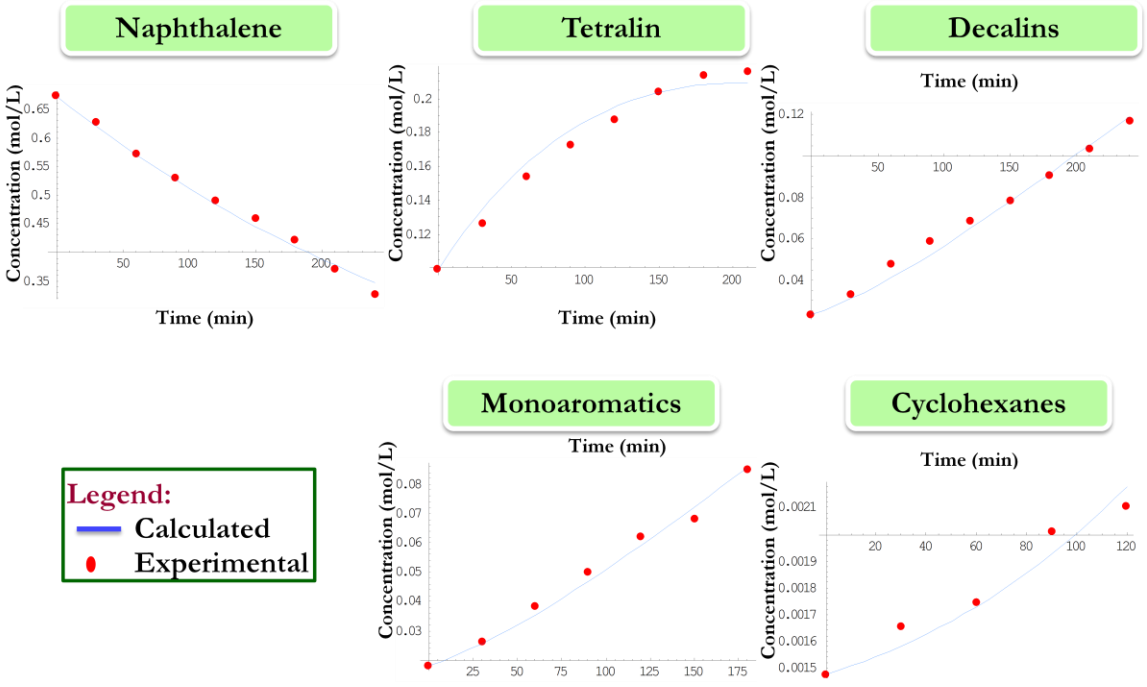


**Figure 4.24 Experimental versus calculated data for RuPdECY-4B**

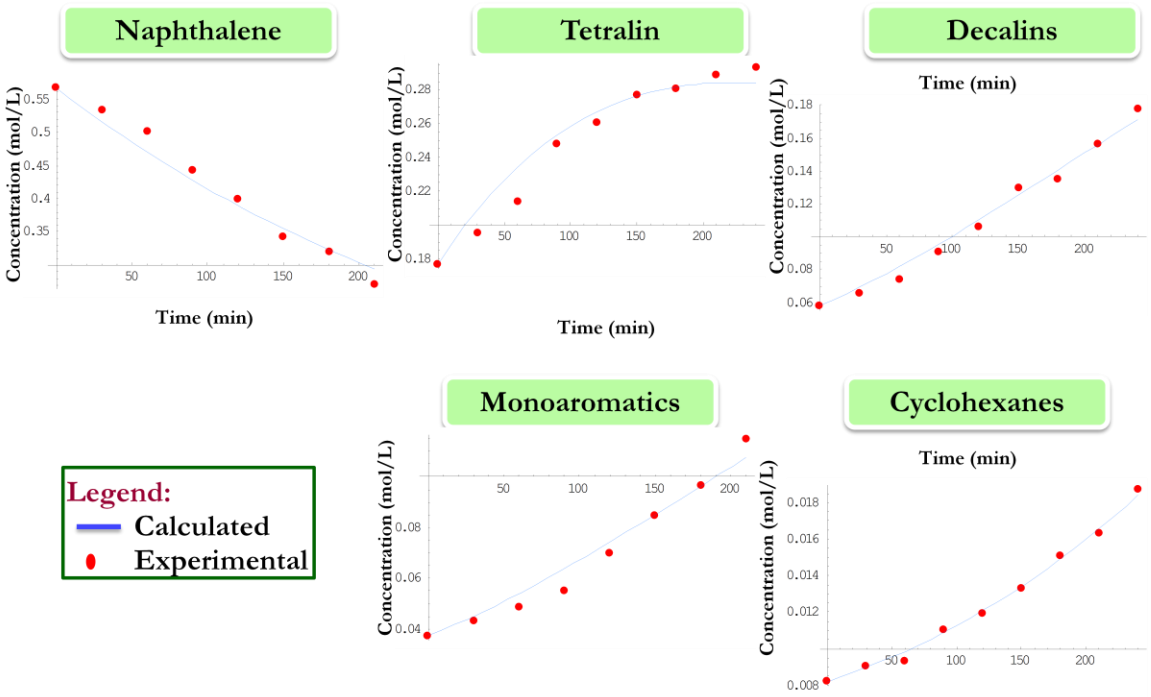


**Figure 4.25 Experimental versus calculated data for RuPd-$Al_2O_3$_YD1**

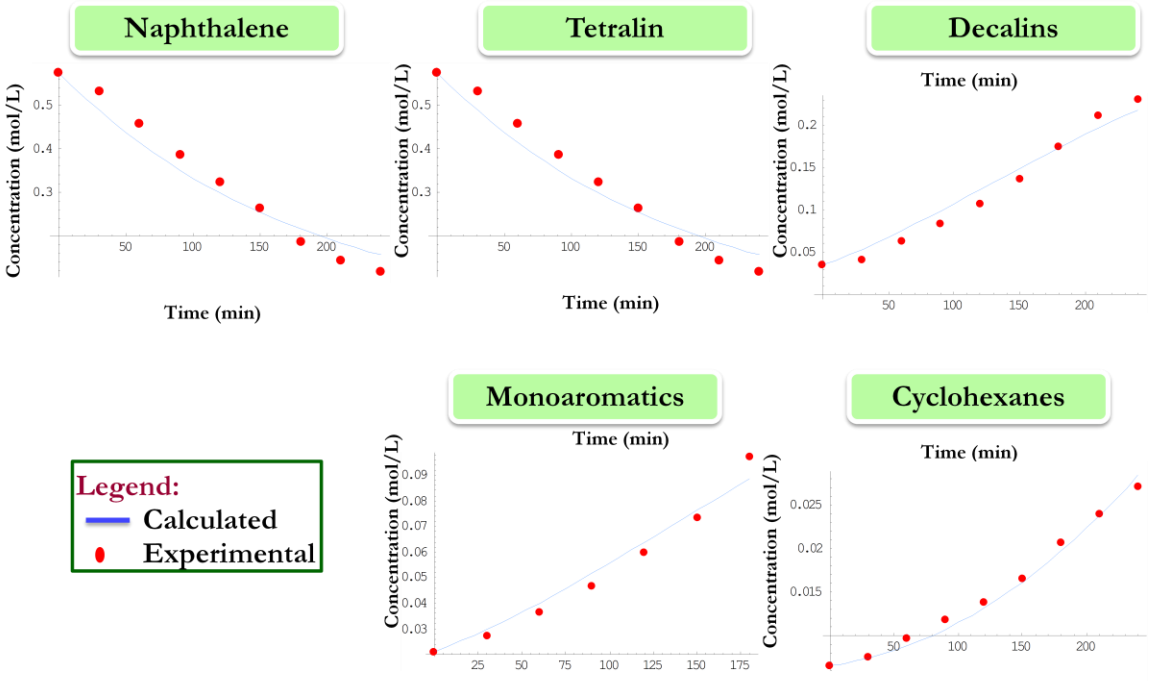


**Figure 4.26 Experimental versus calculated data for RuPd-$Al_2O_3$_YD2**

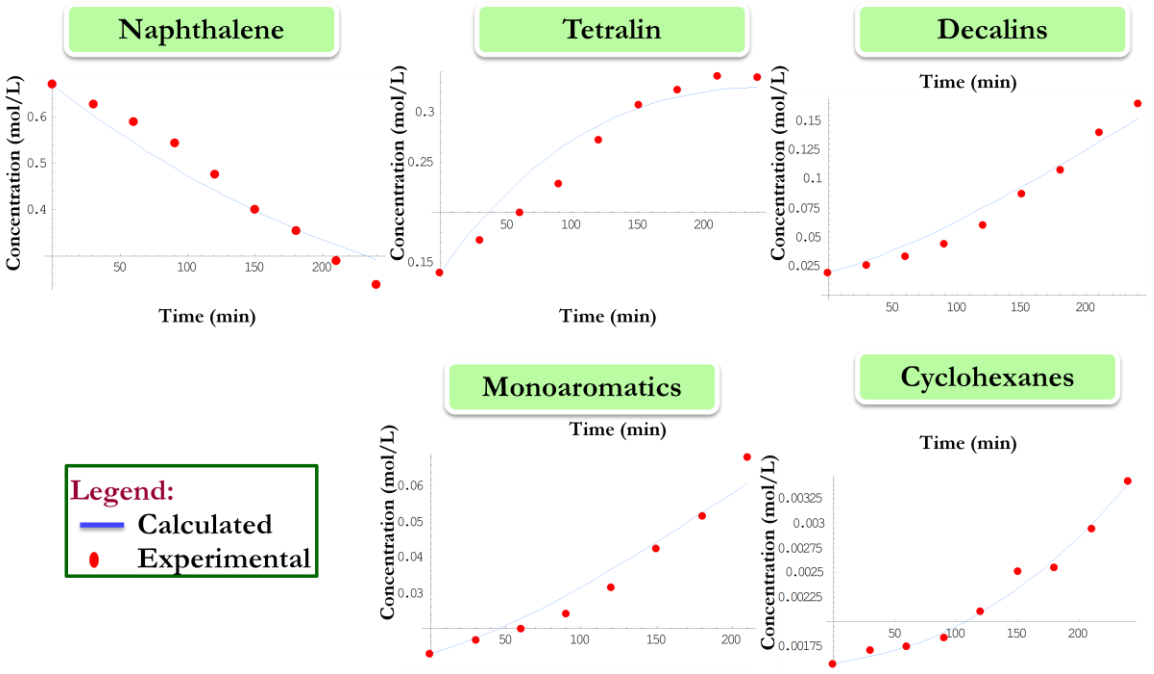


**Figure 4.27 Experimental versus calculated data for RuPd-$Al_2O_3$_YD3**

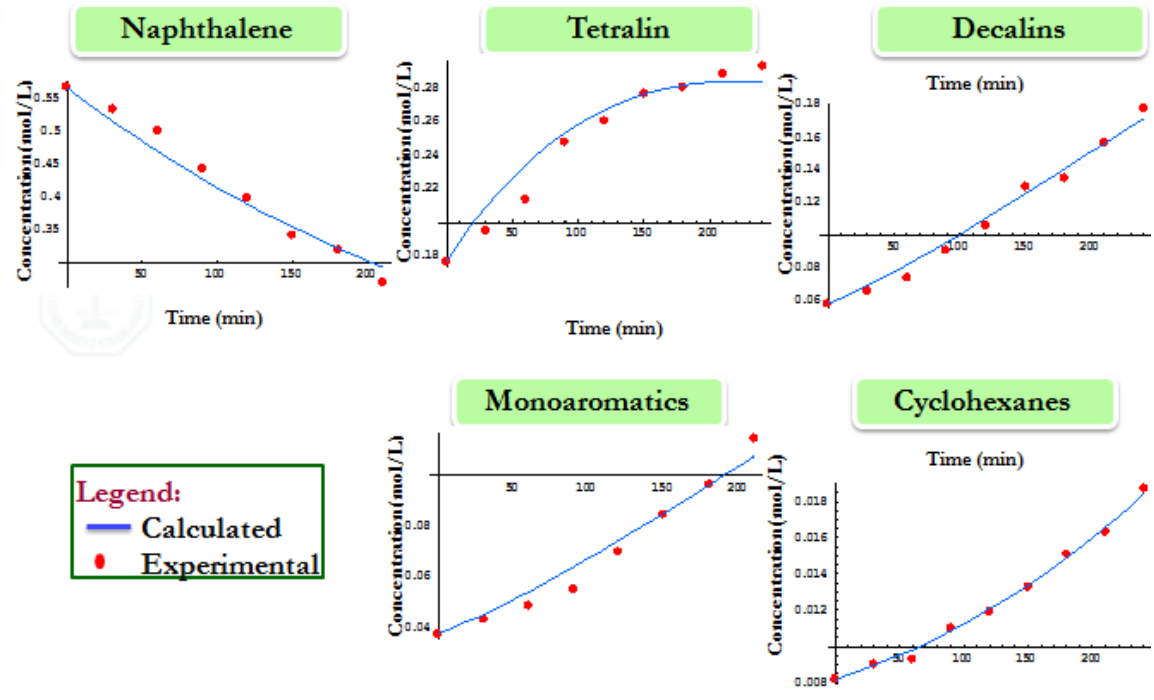


**Figure 4.40 Experimental versus calculated data for RuPd-$Al_2O_3$_YD4**

# CHAPTER 5

# CONCLUSION AND RECOMMENDATIONS

## 5.1 Conclusion

Different series of bimetallic-based catalysts (RuPdECY and RuPd-$Al_2O_3$_YD) composed of varying amounts of Ru-Pd nanoparticles supported on naked and alumina-coated Y zeolite were developed and characterized by a combination of PXRD, SEM, TEM, EDX, ICP-OES, $H_2$ chemisorptions and TPR experiments. The crystalline metal particles are well dispersed and stabilized on the supports. These materials proved to be versatile for the liquid-phase hydrocracking of poly-cyclic aromatic hydrocarbons (naphthalene) and S-heteroaromatics (dibenzothiophene) which are representative components of petroleum-derived fuels, under moderate reaction conditions. The effect of metal loading on conversion of naphthalene was observed to be linear and the nature of supports affects product distribution and yield. The catalysts with naked Y-Zeolite support yielded more cracking products (Monoaromatics and Cyclohexanes) than alumina-coated Y-Zeolite supported catalysts due to their more Bronsted acid sites. On the contrary, the coated series of catalysts were more selective towards hydrogenation products (Tetralin and Decalins). The faster rate of hydrogenation process than cracking further confirmed the higher yield and selectivity and of all the tested catalysts to Tetralin and Decalins. As proved by XRD, all the prepared catalysts are very stable and regenerable which indicate their re-usability without any appreciable loss of catalytic

activity, even in the presence of catalyst's poison-containing dibenzothiophene. With simple improvement in the porosity of the catalyst's support to accommodate bulky molecules, the developed catalysts are future designs of new efficient and poison-resistant noble metal catalyst system for hydrocracking process.

## 5.2 Recommendations

- The series of catalysts prepared can be modified for use as hydrotreating (hydrodesulphurization (HDS) and hydrodenitrogenation (HDN)) catalysts.
- A further kinetics studies be done to investigate the isomerization kinetics especially for cis and trans decalins and ortho, meta and para xylenes.
- These catalysts should be tested on continuous flow reactors for more detailed studies like cycle capacity, regeneration, gases analysis, contact time effects etc.
- The γ-alumina and zeolite ratio should be deeply studied to ensure good metal dispersion and optimum acidity.
- Different metals combinations (e.g. Ir-Pd, Ir-Ru, Ni-Ru, etc.) should be impregnated into the catalysts supports to enhance the hydrogenation and hydrocracking activities.

# Appendices

## Appendix A: Feed preparation

**10 Wt% Naphthalene:**

100 g of naphthalene balanced in 1 liter of Dodecane

**1000 ppm dibenzothiophene (DBT):**

1000 ppm (1000 mg/L):

1 g of DBT in 1 liter of Dodecane

## Appendix B: Sample Calculations

| | | |
|---|---|---|
| Conversion% | = | (amount of aromatic consumed/amount of aromatic)*100 |
| Selectivity% | = | (amount of each product/ total sum of products)* 100 |
| Yield % | = | (amount of each product/ amount of aromatic feed)*100 |
| H/C | = | (H/1) / (C/12) |
| Hydrogenation% | = | (H/C of feed – H/C of product)/(H/C of feed)*100 |

## Appendix C: Rate expressions

- Rate of disappearance of naphthalene; $-d\frac{[Nph]}{dt} = k1[Nph]$
- Rate of formation of Tetralin; $d\frac{[tet]}{dt} = k1[Nph] - (k2 + k3)[tet]$
- Rate of formation of Decalins; $d\frac{[Dec]}{dt} = k2[tet]$- $k4[Dec]$
- Rate of formation of Monoaromatics; $d\frac{[monoaro]}{dt} = k3[tet]$
- Rate of formation of cyclohexanes; $d\frac{[Cyclo]}{dt} = k4[Dec]$

Naphthalene (Nph); tetralin (tet); decalins (Dec); monoaromatics (monoaro); Cyclohexanes (Cyclo)

# References


1. A. Stanislaus, B.H. Cooper, Catal Rev Sci Eng 36 (1994) 75–123.
2. T. Tang, C. Yin, L. Wang, Y. Ji, F. Xiao, J Catal 257 (2008) 125–33.
3. H. H. Schobert, Fuel Process Technol 89 (2008) 364–78.
4. A. S. Nasution, Proc. 5th Int. Semin. New Dev. Engine Oils, Ind. Oils, Fuels Addit., 1985.
5. S. Qader and G. R. Hill, Ind. Eng. Chem. Proc. Des. Dev. 8(1) (1969) 89.
7. F. Y. A. El-Kady, Ind. J. Tech. 17 (1979) 176
8. J. Scherzer, A. J. Gruia, Hydrocracking Science and Technology; 1996 by Marcel Dekker Inc.
9. B. E. Stangeland, Ind. Eng. Chem. Proc. Des. Dev. 13:71 (1974).
10. B.W. Wojciechowski, A. Corma, Catalytic cracking, catalysts chemistry and kinetics, Marcel Dekkar, New York ,1986.
11. M. Seredych, J. Lison, U. Jans, T. J. Bandosz, Carbon 47 (2009) 2491–2500.
12. K.G. Knudsen, B. H. Cooper, and H. Topsoe, Applied Catalysis A: General, 189 (1999) 205-215.
13. D. Chadwick, and M. Breysse, Journal of Catalysis 71 (1981) 226-227.
14. V. Calemma, M.Ferrari, S. Rabl, J. Weitkamp, Fuel 111 (2013) 763-770.

15. X. Liu, K. J. Smith, Applied Catalysis A: General 335(2008) 230-240.

16. M. Fang, R. A. Sanchez-Delgado, Journal of Catalysis 311 (2014) 357-68.

17. S. Jongpatiwut, Z. Li, D. E. Resasco, W. E.Alvarez, E. L. Sughrue, G. W. Dodwell. Appl Catal A 262 (2004) 241-253.

18. Y. Choi, J. Lee, J. Shin, S. Lee, D. Kim, J. K. Lee, Applied Catalysis A: General 492 (2015) 140-150.

19. J. –I. Park, J. K. Lee, J. Miyawaki, Y. K. Kim, S. H. Yoon, I. Mochida, Fuel 90 (2011) 182-189.

20. D. Eliche-Quesada, J.M. Merida-Robles, E. Rodriguez-Castellon, Applied Catalysis B: Environmental 65 (2006) 118-126.

21. S. Ahmed, A. Hassan, K. Alam, M. A. Al-Shalabi, T. Inui, Pakistan Journal of Applied Sciences 2(11) (2002) 1034-1038.

22. J. P. Franck, J. F. Le Page; US7658836 B2 (2010).

23. M. R. Gray, F. Khorasheh, and S. E. Wanke; The role of catalyst in hydrocracking of residues from Alberta bitumens, Department of Chemical Engineering, University of Alberta T6G 2G6 (1994) 384.

24. W. M. H. Sachtler, A. Y. Stakheev, Catal Today 12 (1992) 283–295.

*25.* S. D. Lin, M. A. Vannice. J Catal 143 (1993) 539–553.

26. M. Bouchy, S. Peureux-Denys, P. Dufresne, S. Kasztelan, Ind Eng Chem Res 32 (1993) 1592–1602.

27. M. Chareonpanic, A. Tomita, Energy Fuel 8 (1994) 1522–3.

28. M. Chareonpanich, Z. Zhang, A. Tomita, Energy Fuel 10 (1996) 927–931.

29. A. Corma, A. Martinez, V. Martinez-Soria, J Catal 200 (2001) 259–269.

30. Y. Kim, G. Yun, Y. Lee, Catal Comm 45 (2014) 133-138.

31. H. Topsoe, B. Ckausen, R. Candia, C. Wivel and S. Morup, Journal of Catalysis 68 (1981) 433.

32. C. Wivel, R. Candia, B. Clausen, S. Morup and H. Topsoe, Journal of Catalysis 68 (1981) 453.

33. H. Topose, B. Clausen and F. Massoth, Hydrotreating Catalysis: Science and Technology, Springer-Verlag, Berlin (1996).

34. E. Hensen, J. Lardinois, H. de Beer, V. H. J., J. Veen and V. Santen, J. Catal, 187 (1999) 95.

35. R. A. Khan; Metal Incorporation in MCM-41 for HDS; M. S. Thesis, King Fahd University of Petroleum and Minerals 2001-2002.

36. W. Zamechek, R. G. Pankhurst, in Proceedings of the International ICP Winter Conference, San Juan, Puerto Rico, 1980, Heyden Press, pg 121

37. B.C. Lippens, J.H. de Boer, J. Catal. 4 (1965) 319.

38. E.P. Barret, L.J. Joyner, P.H. Halenda, J. Am. Chem. Soc. 73 (1951) 373.

39. Y. Zhang, Y. Luo, W. Wu, S. Zhao,Y. Long, Energy fuels 28 (2014) 3129−3137.

40. C. Song, X. Ma, Appl Catal B 41 (2003) 207–38.

41. J. Park, L. Ji, J. Miyawaki, Y. Kim, S. Yoon, I. Mochida, Fuel 90 (2011) 182–189.

42. M. X. Du, Z. F. Qin, H. Ge, X. K. Li, Z. J. Lu, J. G. Wang. Fuel Process Technol 91 (2010) 1655–61.

43. S. Ahmed, S. Ali, K. Alam, S. Hamid; Arabian Journal for Science and Engineering 24 (1999) 71-82.

44. B. Pawelec, R. Mariscal, R. M. Navarro. Appl Catal A 225 (2002) 223–237.

45. C. N. Satterfield, Heterogeneous catalysis in industrial practice, Vol. 2, McGraw- Hill International Editions, 1993.

46. T. He, Y. Wang, P. Miao, J. Li, J. Wu, Y. Fang, Fuel 106 (2013) 365-371.

47. T. Kabe, W. Qian, S. Ogawa, A. Ishihara, J. Catal. 143 (1993) 239

# Vitae


Name :Taye Damola Shuaib

Nationality :Nigerian

Date of Birth :3/27/1986

Email :damolataye@gmail.com

Address :Offa, Kwara, Nigeria


**Academic Background**

**2015**: King Fahd University of Petroleum and Minerals (KFUPM), Dhahran, KSA.

M.Sc. Chemistry

**2010**: Federal University of Technology, Minna, Nigeria

Bachelor of Technology in Chemistry

**2004**: The Federal Polytechnic, Bida, Nigeria

National Diploma in Chemical Engineering

**Professional Affliations**

- Chemical Society of Nigeria (CSN);
- American Chemical Society (ACS);
- Saudi Arabian International Chemical Sciences Chapter of American Chemical Society (SAICSC-ACS).

**Conference Papers/ Thesis Works**

**A1** T. A. Saleh, **T.D. Shuaib**. Evaluation of carbon nanospheres decorated with nanoparticles for adsorptive desulfurization, 249th ACS National Meeting & Exposition, Denver, CO, United States, March 22-26, 2015, ENFL-23.

**A2** **T. D. Shuaib**, T. A. Saleh. Cost-effective carbon nanospheres decorated with nanoparticles for adsorptive desulfurization. Applied Functional Material Conference; ACS/KAUST, October 2014, Thuwal, Saudi Arabia.

**A3** **Book Chapters:**

- **T. D. Shuaib**, T. A. Saleh, M. A. Al-Daous. Carbon-based nanomaterials and nanocomposites for desulfurization: classification and evaluation. IGI Global Publisher, PA 17033, USA, *Accepted* April, 2015
- G. I. Danmaliki, **T. D. Shuaib**, T. A. Saleh. Nanomaterials and nanocomposites in adsorptive desulfurization: from synthesis to application. IGI Global Publisher, PA 17033, USA, *Accepted* April, 2015

**B1** **T. D. Shuaib**. Synthesis, characterization and application of bimetallic-based nanocomposites for hydrocracking of naphthalene (M.Sc. Thesis, KFUPM, May, 2015

**B2** **T. D. Shuaib**. Antibacterial Efficacy of the Pigmentend and Non-Pigmented Leaf Extracts of '*Alstonia boonei'* de Wild B. Sc. Thesis, Federal University of Technology, Minna, Nigeria. October, 2010

**B3** **T. D. Shuaib**. Evaluation of stage-wise liquid-liquid extraction equipment (Armfield, UK), National Diploma Thesis, Federal Polytechnic, Bida, Nigeria. October, 2004

## Honor & Award

- Ministry of Higher Education Postgraduate Scholarship (M.Sc), KFUPM, Dhahran, Kingdom of Saudi Arabia
- Federal Government of Nigeria Undergraduate Scholarship (2009-2011), FUT, Minna, Nigeria